Answer to Interactive Comment by Adrian Tuck

June 11, 2019

We thank Adrian Tuck for his valuable comments, that helped us to improve the manuscript. Our answers are given below. The original comment is repeated **bold**, changes in the manuscript text are printed in *italic*.

This is a thorough and interesting paper on an important topic. I have some brief comments: the phenomenon has been observed in the Antarctic too, consistent with the notion that the conditions in the outer vortex there in 1987 resembled the inner Arctic vortex as regards potential for PSC formation. The effect was indeed observed in https://doi.org/10.1029/GL017i00453 from the DC-8 in the Arctic winter of 1988/89. Its occurrence in the Antarctic is discussed in https://doi.org/10.1002/qj.49712353702.

Thank you for pointing us to this interesting aspect. We added citations of both studies to the manuscript and removed the wording “for the first time” from the abstract and conclusion; while GLORIA in fact provides a broad two-dimensional perspective of nitrification of the LMS for the first time, our wording should not be misinterpreted.

Answer to Referee Comment 1

June 11, 2019

We thank referee 1 for valuable comments and suggestions. Our answers are given below. The original referee comment is repeated in **bold**, changes in the manuscript text are printed in *italic*.

General Comments: The authors have reported the observed HNO3 (and O3) from~8km up to 14 km from GLORIA during the PGS aircraft campaign took place from December 2015 to March 2016. The unique aircraft data will be useful for the atmospheric chemistry community. They have mainly focused on four flights data and also used a chemical transport model CLaMS to investigate the nitrification of the lowermost stratosphere for Arctic winter 2015/16. It is clearly shown that there are still large variabilities of measured HNO3 (and O3) in the LMS along the flight track and CLaMS seems to simulate HNO3 quite well though the model is not perfect to capture some fine structures and also underestimates the observed HNO3. Therefore, the authors have also done four sensitivity experiments to try to understand the discrepancies. Overall, the manuscript is well structured. The data analysis and model results are reasonable.

We thank referee 1 for this positive statement.

However, there are some important messages still missing or misleading in the current version. These need to be clarified.

Specific Comments:

1) Selection of aircraft data. It has been mentioned that 18 research flights were carried out between December 2015 and March 2016, but only five flights data are used. Some of other aircraft data may be not suitable for this work, but the authors have not mentioned why they chose these specific 4-5 flights data?

We added information on the flight selection in section 2:

The selection of the flight data was guided by the availability of long continuous "chemistry mode" measurements (see Sect. 2.2) in order to show how patterns in the lowermost stratospheric HNO_3 distribution change during the winter. We furthermore focus on flights in January, where PSCs extended down to the LMS and where the most notable changes are found in the observed HNO_3 distributions. Since we use ozone as a stratospheric tracer to quantify nitrification, flights in January are preferable since only little chemical ozone loss was diagnosed at this time of the winter when compared to February and March (see Johansson et al., 2019). Further GLORIA "chemistry mode" observations can be found in the supplementary information of Johansson et al. (2018) and at the HALO Database (https://halo-db.pa.op.dlr.de/).

2) ClONO2. I think the comparison of ClONO2 between GLORIA and CLaMS would help since GLORIA has also measured ClONO2 (Johansson et al., 2019) and CLaMS simulates ClONO2.

We agree that a comparison of $ClONO_2$ would be of interesting since this species also contributes significantly to NO_y. This aspect is part of the study by Johansson et al. (2019). We added the reference to this study in the manuscript (Page 3, Lines 26-28).

3) Abstract is not well written and some key points are not supported anywhere (for example the sentence in Lines 10-11,

Here we refer to P7/L29-34 and P16/L23-24 of the original manuscript in ACPD where the statements in lines 10-11 are discussed.

I am also not sure if the conclusion in the Lines 11-12 is a fair statement because other satellite has measured HNO3 in this region).

While we agree that other observations (in situ and satellite, see introduction) observed significant nitrification in the LMS region before, we are not aware of any studies reporting such high levels of HNO3 within the LMS due to nitrification as reported here. However, we would like to mention the separate study by Ziereis et al., which addresses this aspect using in situ observations during the same winter. However, we agree that this statement is somewhat strong and modified the abstract as follows:
Overall, extensive nitrification of the LMS between 5.0 ppbv and 7.0 ppbv at potential temperature levels between 350 and 380 K is estimated. ~~This extent of nitrification has never been observed before in the Arctic lowermost stratosphere.~~

What are missing in CLaMS when the authors conclude the model underestimates....(Lines 15-16).

The reasons for this deficiencies in the model are yet unclear. It should be noted that the distribution of tracers depends critically on vertical transport and that the vertical velocities are difficult to model. Another sources of uncertainty are the physical parametrisations and their implementation in the model. Therefore, a point-to-point agreement between model and observations is not expected. However, recent studies (Grooß,2018; Tritscher, 2019) showed that the in principle, the vertical HNO_3 (and H_2O) redistribution is reproduced well.

What is the implication for this work to improve HNO3 simulation in the lowermost stratosphere though some has mentioned in the Introduction?

There is no obvious fix. However, we point out a possible strategy assess our model understanding. We stated in the introduction that we test how well different parameterizations within the model reproduce the GLORIA observations. Based on our results we conclude that the sensitivity simulations show differences and lead to a sometimes improved agreement. However, no sensitivity simulation can be identified that generally improves the model. Therefore, we conclude that more extensive modifications of the model parameters addressed by our study are required and/or that important processes are still missing in the model. For clarification, we modified the abstract at P1/L19ff as follows:

… waves) slightly improve the agreement with the GLORIA observations of individual flights. However, no parameter could be isolated which results in a general improvement for all flights. Therefore, we conclude that a more comprehensive change in the model representations is required. Still, the sensitivity simulations suggest that details of particle microphysics play a significant role for…

4) Section 3.2 (Page 5). I am confused with the description. If CLaMS can save daily output at 12:00 UTC, why it can not save the model output along flight track (time, locations etc)? I am not sure why CLaMS needs to re-run forward/backward trajectory for the flight track though I understand CLaMS is based on trajectory calculations..

Using a standard forward integration, interpolation would always be required. Regardless how the flight paths are constructed, there would be no guarantee for a trajectory ending on the flight path at the right time. Certainly it could be done online with a slightly improved temporal resolution; however, the standard product for a longer term forward integration is stored in snapshots and processed afterwards.

5) Results explanation. Sometimes it is very hard to follow. For example, Page 7 Lines 9-10. Maybe the coarse vertical resolution is one factor. That will be easier to confirm by increasing the model vertical resolution in the LMS.

We investigated this effect and could not confirm the coarse vertical resolution as a dominating factor. However, since this flight was removed in context of suggestions by referee 2, this aspect is not mentioned any more in the revised manuscript.

Pages 9 and 10: What are the key points here? Sorry it is hard to understand the Lines 1-2 in Page 10.

We revised the discussion of the vertical cross sections to better highlight the key points (see revised manuscript). Further, we removed the statement given in lines 1-2 (see comments to referee 2).

Lines 15-18 in Page 12. Not so sure the points of the estimation of lower limit nitrification (though there is an almost linear relationship from the reference in Figure 5).

For clarification, in the revised figure (now Fig. 4) we constructed the same correlation neglecting a potential ozone loss of 15 % (i.e. the ozone mixing rations are scaled accordingly), which now clearly shows potential impacts of ozone loss on the presented tracer-tracer analysis.

6) Sensitivity experiments in the Page 13. The descriptions of the model sensitivity experiments are too general. Some of these can only be understandable by the people who are familiar with CLaMS. For example, 'ice settling' simulation, the authors just have one extra criteria to consider in the model (Line 17-18), but we don't know how settling velocity is calculated in the standard CLaMS model. 1.5 times settling velocity for the whole altitude range or something like that needs to add.

We added a reference for the settling velocity and changed the manuscript for clarification:

Therefore in the 'ice settling' simulation the computed ice settling velocity (computed as described by Tritscher et al., 2019) was increased by a factor of 1.5 at all locations where the saturation ratio of ice, S_{ice}, is larger than 1.2.

For the temperature offset, why decrease global temperature by 1K rather than 1.5 or 2 K? Just simple say "NAT formation is T dependent" seems not enough.

We chose this sensitivity test based on the study by Hoffman et al., 2017 [ACP 17, 10.5194/acp-17-8045-2017, 2017]. This study found that temperatures from ERA Interim have a bias of 0.8K in comparison with those from Concordiasi long-duration balloon measurements in the Antarctic. For MERRA-2 they find a bias of 1K. We assumed that errors in the Arctic are unlikely to be much larger. Therefore, this number seems useful to us to investigate the impact of a potential temperature bias.

7) Discussion and Conclusion. Can you add more why the nitrification for Arctic winter2015/16 has much more than previous work as you mentioned in the Lines 20-26 in the Page 17?

We added following sentences to the manuscript:

During the Arctic winter 2015/16 exceptionally low stratospheric temperatures occurred and the vortex was sufficiently stable to allow formation of PSCs down to lowest stratospheric altitudes. Those conditions were the prerequisites for the strong nitrification observed and presented here.

Technical corrections:

1) Abstract, Page 1 Line 1, change "cold" to "low".

We changed the manuscript according to the referee's suggestion.

2) Page 1Line 5, why it is only spatial resolution? Does high temporal resolution matter for this case?

We emphasize the aspect of high spatial resolution, since our measurement technique allows particularly for a high spatial resolution. With regard to temporal resolution, the GLORIA data show continuous observations (i.e. 1 profile is measured in ~13 s), but of different air masses along entire flights or flight sections over periods of several hours. Thus we are focusing on overall conditions that are representative for several hours, while fast developments (i.e. at timescales of seconds or minutes) are not in focus of our study and would require a different experimental/flight design (e.g. "self-match flights" or a slowly moving carrier such as a balloon).

3) Page 1 Line 9. Are you sure about 11 pbbv of HNO3 is observed at 11 km from GLORIA? The only one I can see from Figures 4 and 5 but it occurs above 12 or13 km (?)

Thank you for pointing this out. We agree and changed it to 12 km.

4) Page 3 Line 7-8. What do you mean "mesoscale temperature is not well known"?

We changed the manuscript to: *mesoscale temperature modulations (e.g. by gravity waves) are…*

5) Page 3 Lines 18-20. This is too general.

We changed the manuscript to: *We compare the GLORIA data with simulations by the Chemical Lagrangian Model of the Stratosphere (CLaMS; Grooß et al., 2014, references therein). To test how well different parametrizations within the same model reproduce the GLORIA observations, four sensitivity studies were performed. Those sensitivity simulations investigated the impact of (i) enhanced sedimentation rates in case of ice supersaturation, (ii) a global temperature offset, (iii) modified growth rates and (iv) temperature fluctuations.*

6) Page 4 Line 2. "spectra and spectra"?

For better understanding we rephrased to: *… are transformed into spectra. The spectra from horizontal detector rows …*

7) Page 4 Line 25-26. A reference is needed. Is the same reference as Tritscher et al. (2018)?

Yes it is, we added the reference to the manuscript.

8) Page 5 Line 20. Add a reference for MERRA2. Why not to use ECMWF ERA interim because you have also done the model simulations based on the meteorological conditions.

We added a reference for MERRA -2. Data products from MERRA-2 were available, too. However, since we assume the MERRA2 and ECMWF datasets to be of comparable quality, we used both datasets.

9) Page 5 Line 22. Better to use "x" rather than . after"1.2"

We changed the manuscript according to the referee's suggestion.

10) Page 6 Line 3. Better to add an altitude range after 1.2 ppmv.

We removed this flight from the manuscript, based on the suggestions of referee 2.

11) Page 7Lines 8-9. Can you make "the enhancement at low altitude" clear? Is it enhancement of HNO3 inside the vortex region compared with outside vortex. Or you mean 2-3 ppbv HNO3 inside the vortex.

We removed this flight from the manuscript, based on the suggestions of referee 2.

12) Page 12. The unit in the text should be consistent with the figure

We changed the units of the figure to ppmv.

Answer to Referee Comment 2

June 11, 2019

We thank referee 2 for valuable comments and suggestions. Our answers are given below. The original referee comment is repeated in **bold**, changes in the manuscript text are printed in *italic*.

This paper presents interesting observations of hno3 from aircraft observations in the Arctic winter of 2016 indicating nitrification of the Arctic polar vortex in the 10-14 km range, the maximum altitude of the observations. While the observations are of interest and the overall analysis convincing, that nitrification of the lower most stratosphere occurred, the paper is poorly written, much too long, and should not be accepted in this form. Throughout the descriptions of the individual flights, which are used to introduce the observations, the authors claim that the observations show redistribution, enhanced hno3 layers and nitrification. This is before the methods are explained, or the reference profiles discussed. The reader has to guess how these conclusions are made. The description of the figures often resorts to a recitation of numbers in the figures. The authors specify vortex air in the figures by stating what is not vortex air. Figure caption 2 confuses by not describing the panels in order. Waypoints marked in figures are not used. Reference is made to NOy*, but it is not used further, or defined. The claims of "distinct differences," with some of the CLAMS sensitivity tests, are not well supported by the figures. The paper could be published, but only after major revision.

We thank referee 2 for pointing out that the presented observations are of interest and for the very helpful and constructive criticism which lead to major changes described under the specific items below.

The analysis should begin by describing that ozone will be used as a tracer for the air sampled and to describe why that works for 2016. Thus the majority of section 5 should appear before any aircraft data are shown. Only two detailed aircraft profiles need to be shown, first the reference profile in December which currently is not shown, and an example of the measurements in January.

We agree that the structure of our study is not stated clear enough at the beginning and understand now that our intentions are somewhat difficult to extract. As correctly pointed out by referee 2, the central result is the quantification of nitrification of the LMS ("research question 2"). However, our goal is also to show how 2-dimensional vertical HNO_3 distributions in the LMS are structured at different stages of the winter and how these patters compare with an established chemical transport model ("research question 1"). For clarification, we modified the manuscript as follows:

- *How are HNO_3 distributions structured in the LMS during the course of the cold Arctic winter 2014/16? How do HNO_3 distributions, which are affected by nitrification, compare with the stratospheric tracer ozone? How do observed small-scale spatial patters compare with a model (CLaMS)?*
- *Do tracer-tracer correlations constructed from GLORIA HNO_3 and O_3 indicate nitrification of the LMS? How does nitrification inferred from the GLORIA observations compare with that inferred from CLaMS? Can we identify a critical model parameter which results in a significant overall improvement of the agreement?*

Thus, our manuscript is structured in the following way: In section 2, we introduce the measurement campaign and the data used. In section 3, we introduce the specific characteristics of the data products and the methods and approach of the analysis.

In section 4, we present GLORIA cross-sections of HNO_3 and CLaMS simulations to address the first block of research questions. Thereby, we discuss observed patterns in the HNO_3 distribution only qualitatively; here, the underlying assumption is that nitrified regions can be identified as patterns differing qualitatively from patterns in the ozone distribution, which experiences no vertical redistribution associated with PSCs.

In section 5, we finally use the previously introduced GLORIA data to derive nitrification of the LMS using tracer-tracer correlations, and test the sensitivity of the model to modifications of different parameters (second block of research questions).

In our opinion, the discussion of individual flights provides valuable insights into the quality of the data and how nitrification patterns are structured in the LMS. Therefore, we think that the results presented in section 4 are the prerequisite for the analysis presented in section 5.

We agree that the method of quantification of nitrification for research question 2 should be provided already in the methods section and revised the manuscript accordingly. The method is now explained in the new section 3.4.

These two examples are enough to set the stage for the relative normalized frequency distribution (RNFD) discussion, and Figure 6, which is the key figure of the paper. A figure showing an example of RNFDs would also be of interest. While the authors seem to be keen on showing all of the aircraft data in detail, this really distracts from the main point of the paper. The authors should find another venue to do that and to stick here to the science which can obtained from the data.

We agree that the presentation of a larger number of flights draws away the reader's attention from the key results and removed flight 6 from the revised manuscript. However, we think that the remaining flights are important to address the first block of research questions. Furthermore, we now provide a rationale for the flight selection (see comments to referee 1). In addition, we added a figure (new Figure 1) showing an exemplary RNFD together with the single correlation points.

Further detailed comments follow by page and line number.

3.6-8 What is meant by stating that "the vertical HNO3 redistribution may be saturated"? How is a vertical redistribution saturated?

We changed the manuscript to:

At a later time, ~~the vertical HNO$_3$ redistribution may be saturated as due to the lower HNO$_3$ mixing ratio, no additional NAT particles can be nucleated.~~ in order to nucleate new NAT particles in denitrified air, lower temperatures are needed because of the already decreased HNO_3 mixing ratios. This results in a maximum potential denitrification for a given temperature. .

5.28-29 and Fig 1 caption. In the text "the identified vortex region (indicated by non-shaded areas in Fig. 1a)" and the figure caption, "light grey shading: areas that are not associated with the polar vortex", are at best confusing and at worst contradictory.

We removed this flight as according to the referee's suggestion.

The figure caption's version is more consistent with the figure, but then there is a meandering split of the vortex into a western and eastern half. The uniform width of this split seems to indicate more than a filament of non-vortex air.

We removed this flight as according to the referee's suggestion.

6.1-2 "Only above the British Isles, southern Scandinavia and north-west of Norway patches of air masses do not fulfil this filter criterion." How is the reader to interpret this statement? Is it an apology that these regions aren't also included as vortex air, thus doubting the Nash criterion? Is "southern Scandinavia" meant to indicate the southern Baltic Sea? The aforementioned region of air nearly splitting the vortex cannot be characterized as "patches of air masses". And with the criterion indicated as vortex a majority of the a/c observations are in this "patch".

We removed this flight as according to the referee's suggestion.

6.10-7.2 "In summary, the observed HNO3 structures exhibit a much larger spatial variability than those observed in the ozone distribution, indicating their formation due to redistribution processes." This statement is not acceptable. First the figure does not show a "much larger spatial variability in HNO3 than in ozone. Between 11:30 and13:00 in the flight data, both gases vary: HNO3 from 3-7 ppbv, a factor of 2, ozone from 0.4 -1.2 ppmv, a factor of 3. Second if there were a difference how does that immediately lead to the conclusion of a redistribution process? There must be some additional explanation to make this leap this early in the paper.

We removed this flight as according to the referee's suggestion.

7.11-12 "during in..." "Nash criterion, a relatively"

Done.

7.13 redundant with 7.11, please don't repeat.

We have deleted this sentence and added PSC occurrence to 7.13

7.15-16 "a number of GLORIA observations where sorted out by cloud-filtering" What does this mean? Sorted out and put where? Do the authors mean remove? I do not understand what sorting out means.

We changed **sorted out** to *removed*.

7.20 NOy* has not been explained and there is no reference and it is not used again. Is it important?

We changed "NO_y*" to "total NO_y"

7.20-23 What is particulate HNO3? Perhaps these are particles vaporized in an inlet and the hno3 gas measured, or ???

Yes, NOy containing particles were vaporized and measured as gas phase equivalent.

Why are the data not corrected for enhancement efficiency, insufficient information, small correction,...? Is it important that they are not corrected?

They are not corrected because of insufficient information on this parameter for this specific flight configuration. Here we use the data only to show qualitatively that NO_y-containing PSC particles were present at flight altitude. This information can be clearly inferred from the data, despite the uncertainty of the inferred absolute values of particulate NO_y which rely on assumptions.

Why do the presence of HNO3 containing PSC particles need to be confirmed? Confirming compared to what? What other kind of PSC particles could be present besides hno3-containing particles?

The presence of HNO_3-containg particles needs to be confirmed to distinguish from potential cirrus cloud particles. Here, we aim at showing (i) that particles (i.e. a PSC) are indeed found at these low altitudes and (ii) that the particles contain NOy and are therefore likely to be linked with designated nitrification patterns seen in the GLORIA observations.

The first particle maximum doesn't coincided with a GLORIA maximum, but should it, if the hno3 has condensed?

In a simplified view, maxima in particulate NO_y should coincide with regions of low gas-phase HNO_3 (GLORIA), as particulate NO_y that is transported downward during denitrification from higher layers is still in the solid phase. However, this simplified assumption does not necessarily hold depending on the previous de/nitrification history of the observed air masses. Therefore, here our main point is that we find NO_y-containing particles (probably transported downward by gravitational settling during the denitrification of higher layers) in the vicinity of highly structured local maxima of NO_y (which differ from patterns of the "dynamical" tracer O_3), which suggests that nitrification was going on in the observed air masses.

7.30 What is meant by "band-like structures"?

By band –like structures we referred to the connected/coherent structures tilted with altitude. We changed **band-like structures** to *coherent structures tilted with altitude* in the manuscript.

7.33 "distribution, indicating their formation by redistribution of HNO3" The authors again jump to their major conclusion without presenting any reasons.

The indication of nitrification is based on the assumption that ozone and HNO_3 are affected by the same dynamical processes. We added an explanation at the beginning of the section to support this conclusion (Page 7, Lines 11-16):

The observed patterns in the HNO_3 distributions are compared with the observed patterns in the ozone distribution. Since ozone and HNO_3 are effected by the same dynamical processes, the different patterns in the observed distributions are likely caused by processes that effect only one species (i.e. nitrification due to sublimation of NO_y-containing particles sedimented from higher altitudes). Therefore, the local HNO_3 enhancements seen in comparing adjacent air masses at a given height level and the deviations of their pattern from the pattern seen in the ozone distribution are interpreted qualitatively as a result of nitrification.

Although we are convinced that strong hints for nitrification can be inferred from qualitative comparing the GLORIA HNO_3 and ozone distributions (which provide the foundation for the subsequent quantitative tracer-tracer analysis), we agree that the main conclusion should not be stated already here and therefore changed "indicated" to "*suggest*".

7.34-35 Here for the first time the authors make an argument for their conclusion, but it is very brief and none of their data has included temperature relative to equilibrium temperatures with respect to NAT. Such information would help the reader understand why in some regions there are particles and in other regions gas phase hno3? In the regions where GLORIA data are shown, should the reader assume these are cloudfree?

Prior to the retrieval process of trace gases, the GLORIA data are cloud-filtered according to the cloud index method by Spang et al. (2004) since too strongly influenced spectra by clouds would lead to larger errors in derived trace gas abundances. However, this is a qualitative method for cloud filtering, and under conditions of low cloud index values (i.e. a high influence of particulates in the spectra, as observed here), the presence of cloud particles at flight altitude cannot be excluded. While the particulate in situ NO_y observations (i.e. measured total NOy=(gas phase+particles evaporated in the

instrument; forward inlet) minus gas phase NO_y (gas phase only, backward inlet) are sensitive to cloud particles, with the GLORIA observations only HNO_3 in gas-phase is derived; however, the simultaneous presence of particulate NOy in the same air volume cannot be excluded.
The GLORIA temperature data (not shown, see supplement to Johansson et al., 2018) indicate temperatures close to the equilibrium temperature of NAT (and well above the equilibrium temperature of ice) in the vicinity of the HNO_3 maxima and where particulate NO_y is detected. Thus, the GLORIA data support the processes of evaporation and persistence of NAT particles at temperatures close to saturation versus the NAT phase. However, the accuracy of the GLORIA temperature observations is not sufficient to explain precisely the observed pattern of particulate NO_Y observations and HNO_3 maxima.

Figure 2 caption. The panels need to be described in the order in which they appear. A figure caption is so readers can understand what is in the figure. Why confuse them by listing the contents of each panel out of the order in which they appear?

We changed this according to the referee's suggestion.

Since the interest is in polar vortex air, why do the authors state, here and elsewhere, what is not polar vortex air, rather than what is polar vortex air?

We changed this according to the referee's suggestion.

8.1-6 While the hno3 mixing ratios for CLAMS agree with GLORIA, CLAMS does not show anything like the altitude tilted features appearing in the hno3 GLORIA data. What particle information does CLAMS contain? Does that reproduce the in situ particle measurements?

The setup of the CLaMS run is focused on the stratospheric composition and the resolution below ~9 km altitude is rather poor. This is one of the reasons, why CLaMS does not show detailed structures below ~8 km altitude. The evaporating HNO_3 from the simulated particles is then distributed within a vertical large grid box and therefore hardly visible.

Figure 3 Why is waypoint A marked on the map and then not on the panels and not mentioned in the text.

Waypoint A is not shown in the panels, since this part of the flight is not shown there. We added this information in the figure caption.

9.8 Why call the hno3 mixing ratios "enhanced" and "strongly enhanced"? This language assumes the authors' pre-determined conclusions prior to the arguments being made. The hno3 mixing ratios are what they are, without this qualifying language.

We removed the distinction between enhanced and strongly enhanced values.

10.1-2 "Since those structures between waypoints C and E vary significantly from those observed in the ozone concentrations they most likely originated from nitrification" Is this now the argument to be pursued, using ozone as a tracer? But in fact Figure panels 3b) and 3c) do not support the statement. The structure and the relative magnitudes of ozone and hno3 are quite similar. How do they "vary significantly"?

When looking closely, different patterns can be identified, e.g. the local HNO_3 minimum (~3 ppbv lower compared to ambient mixing ratios) at flight altitude directly around waypoint D which is not identified in the ozone distribution. However, we agree that this aspect is difficult to extract from the figure and does not need to be pointed out here. We therefore removed this statement.

10.3-4 Now the CLAMS hno3 is "enhanced" even though the maximums and structure of the high hno3 regions do not match the observations. What is the significance of pointing out the very narrow high regions of hno3 in the CLAMS hno3? The last sentence describes well how the model and observations compare.

As described in the previous section, the "enhancement" is based on the comparison with GLORIA observations of HNO_3 mixing ratios in adjacent air masses and at the same potential temperature levels (see potential temperature isolines). Therefore, structured patterns in the HNO_3 distributions inside the LMS at the same potential temperature level and differing from the ozone distribution are likely to be affected by an additional non-dynamical process, i.e. nitrification by sublimation of NO_y-containing particles originating from higher layers.

In the used measurement mode, GLORIA measures a profile about every 13 seconds resulting in more than 250 profiles per hour. Further, the measurements during this flight span several 1000 km. Therefore, regions that appear narrow in the cross sections are still representing areas of several tens to a few 100 km and should not be interpreted as single data outliers.

11.6-9 The enhanced language is used again and the claim of structures indicative of nitrification, as if this point is obvious for almost all of the hno3 values measured by GLORIA greater than some number. Perhaps if the reader were shown "non-enhanced" measurements of hno3 they may agree with the authors about the language, but all we see are hno3 values in the range of 5-10 ppbv pretty much in every flight segment shown.

As described in the previous answer, the "enhancement" is based on the comparison with GLORIA observations of HNO_3 mixing ratios in adjacent air and at the same potential temperature levels.

11.22- It would be helpful to show some of the relative normalized frequency distributions. These could be more interesting for the reader than so many flight profiles, and the pointing out of small features in the flight profiles, which now may be removed as outliers, when the data analysis is finally explained.

We added an example for the relative normalized frequency distribution to the methods section. However, as we stated before, small features in the vertical cross sections stretching over several profiles are still representing several tens to a few hundreds of kilometers and therefore are not due to outliers.

12.5- Here finally information on the reference profile which motivated the previous language about enhancements, etc. is offered to the reader. Considering its importance the paper would be better served by showing this nominal reference data for comparison with the more dynamic data later.

We hope that we could clarify above that the qualitative discussion of nitrification described in the previous sections is not based on this reference profile. The local enhancements described in the previous sections are derived qualitatively by considering modulations in HNO_3 distributions on wide ranges at (i) constant potential temperature levels inside the vortex region and (ii) with the corresponding ozone fields. The HNO_3 and ozone data shown in the cross-section provide the foundation for the quantitative tracer-tracer correlation discussed here. While the slopes of the different overall relative normalized frequency distributions (RNFDs) indicate how the overall nitrification state of the LMS develops during the winter, the widths of the RNFDs show the variability of the nitrification state at the dates of the flights (i.e. simultaneous presence of already nitrified regions and less/non-nitrified regions; these are the "differences " in the patterns seen when comparing the HNO_3 and ozone cross sections).

I am not sure the point of sentences listing the numbers of the maximums. Tables are good for numbers. Text is good for describing general features of the figures such as the progression of the descent of the hno3 over January and how CLAMS doesn't capture this, nor the magnitude of the hno3.the

We changed this paragraph to a more descriptive text for better readability.

12.14 An ozone loss of 15% significantly reduces the nitrification, so it needs to be clarified whether this was possible. Was such ozone loss occurring in the LMS? CLAMS should be able to at least estimate this.

Our assumption of an ozone loss of 15% is based on the study by Johansson et al. (2019), where the ozone loss during the Arctic winter 2015/16 was estimated based on CLaMS calculations.

Additionally, we investigated the ozone depletion in the LMS based on CLaMS (see following Figure1 (not shown in the manuscript)). This shows a good agreement with the 15% that we assumed in our study.

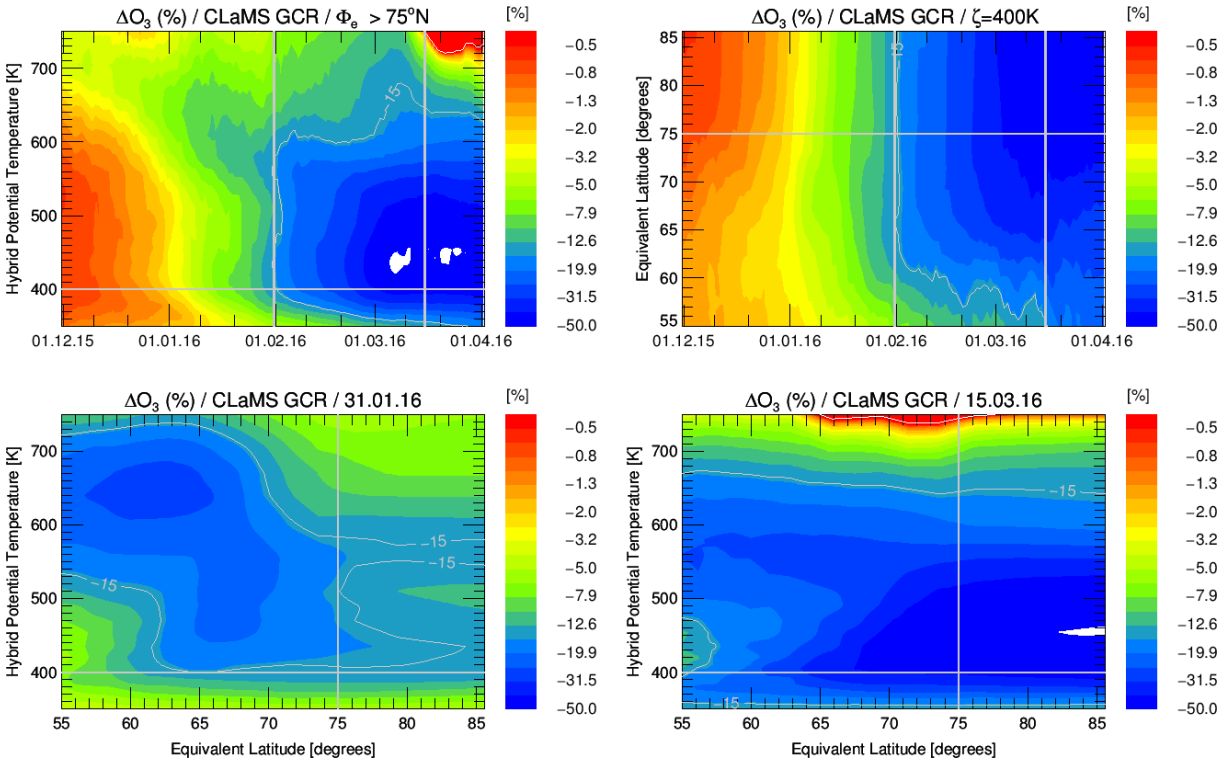

Figure 1: Ozone depletion in the LMS estimated by CLaMS.

For clarification of the given numbers, in the revised figure (now Fig. 4) we constructed the same correlation assuming a potential ozone loss of 15 % (see comments to referee 1).

12.16 I thought the measurements were filtered from non-vortex air in several ways. Are we now to assume that these correlation plots may be affected by non-vortex air?

The measurements were filtered such that non-vortex air was excluded, as described in section 3.3. As we pointed out there, a robust identification of vortex air is difficult in the altitude regions where the measurements were made. Therefore an influence by non-vortex air cannot be excluded entirely.

13.4-9 Another paragraph pointing out the numbers which the reader can more easily obtain from the figure, or if they are important could be put in a table. Text should be reserved for something

more interesting. This whole paragraph and others like it could be mostly removed and the paper would be better for it.

We changed this paragraph to a more descriptive text for better readability.

13.10-12 Yes but CLAMS completely misses the continuing descent of the hno3 observed by GLORIA.

Here, the point addressed by the referee is not clear to us. “Descent” in the sense of “nitrification by sedimented NAT particles” is clearly identified in both the GLORIA and CLaMS data as the change of the ozone-HNO_3 slopes from flight to flight, but the extent is different in the GLORIA data and the simulation (i.e. less nitrification or “slope change” is found in CLaMS data, but the nitrification is not completely missed). On the other hand, “descent” in the sense of “diabatic airmass descent” cannot be read from this plot, as this diabatic airmass descent would affect ozone and HNO3 in the same way and the correlation slope would remain unchanged.

13.27-29 “The comparison is based on the RNFDs depicted for the individual flights in Fig. 6.” And that is all there is to say about the sensitivity analysis of CLAMS compared to the flight data? Amazing, after the paragraph above describing all the different scenarios to test the sensitivity of CLAMS, no discussion of the results which indicate that the CLAMS results are almost insensitive to these perturbations.

This statement was used to refer to Figure 6 which is the basis of the discussion in the following sections 6.1 – 6.4.

As suggested by the referee we decided to remove sections 6.1 – 6.4 and offer a more general discussion in section 6 to the reader (see revised manuscript).

Figure 6 the flight dates should be added to the figure panels for reference later.

We added the flight dates in Figure 6.

13.30-16.6 Without much of a difference observed in the summary RNFD plots for the CLAMS sensitivity tests the authors proceed to discuss the flight 6 cross section and its sensitivity simulation in detail, pointing out fine features/differences in Figure 7. But what is the conclusion reached from this detailed discussion?

As stated before, RNFDs and cross sections offer a different perspective on the data. While RNFDs give a more general picture of the data, the cross-sections give additional information on the representation of spatial fine structures. However, we agree that the observed differences are small and therefore decided to move Figure 7 to the appendix.

Line 14.8, “However, the overall structure in the RNFD is similar to the reference simulation.” Exactly, which is clear from Figure 6a. With this diversion back to detailed discussions of cross sections I gave up on the paper, assuming the same was going to be done for each subsequent flight. Although this is not done, neither is a general discussion of figure 6 offered. Is it really important to go through each model sensitivity difference for each flight when there are so few differences with the reference? A more helpful discussion of the figure would organize it by model sensitivity, and only discuss those sensitivities which make a significant difference with the reference in the direction of the observations. Based on Figure 6 this criteria would shorten the discussion considerably. Figure 7 and the current sections 6.1-6.4 should be removed.

We agree that a discussion based on model sensitivity would be more helpful and therefore changed the manuscript to a more general discussion of Figure 6.

17.11-19 Claiming distinct differences is an overstatement. The improvement of the temperature fluctuation for 31 Jan. is only evidenced by increased hno3 near 800 ppbv, otherwise it matches the CLAMS reference and all simulations lay significantly higher than the observations. The improvements in the T-1K simulation are generally hardly outside the reference except for 20 Jan. The aspherical particle case provides only a slight difference on 12 Jan. If some estimates of precision were placed on the CLAMS reference, most sensitivity simulations would be hardly outside. The sensitivity simulations simply do not support the claim of distinct differences.

We agree that the improvements are small for most of the flights. However, we observe changes for individual flights even though no sensitivity simulation shows a distinct improvement for all flights. Therefore we changed **distinct** to *noticeable*.

Which sensitivity should be chosen to improve the overall agreement with observations over the campaign? There is none.

We agree with this statement. This issue is not solved by this study. We stated in the introduction that we test how well different parameterizations within the model reproduce the GLORIA observations. Based on our results, we conclude that the sensitivity simulations show differences and lead to a sometimes improved comparison. However, no sensitivity simulation can be identified that generally improves the model. Potentially, important processes are still missing in the model, or stronger changes of parameters tested here need to be implemented.

Nitrification of the lowermost stratosphere during the exceptionally cold Arctic winter 2015/16

Marleen Braun[1], Jens-Uwe Grooß[2], Wolfgang Woiwode[1], Sören Johansson[1], Michael Höpfner[1], Felix Friedl-Vallon[1], Hermann Oelhaf[1], Peter Preusse[2], Jörn Ungermann[2], Björn-Martin Sinnhuber[1], Helmut Ziereis[3], and Peter Braesicke[1]

[1]Institute of Meteorology and Climate Research, Karlsruhe Institute of Technology, Karlsruhe, Germany
[2]Institute of Energy- and Climate Research, Stratosphere (IEK-7), Forschungszentrum Jülich, Jülich, Germany
[3]Institute of Atmospheric Physics, German Aerospace Center, Oberpfaffenhofen, Germany

Correspondence: Marleen Braun (marleen.braun@kit.edu)

Abstract. The Arctic winter 2015/16 was characterized by exceptionally ~~cold~~ low stratospheric temperatures, favouring the formation of polar stratospheric clouds (PSCs) from mid-December until the end of February down to low stratospheric altitudes. Observations by GLORIA (Gimballed Limb Observer for Radiance Imaging of the Atmosphere) on HALO (High Altitude and LOng range research aircraft) during the PGS (POLSTRACC/GW-LCYLCE II/SALSA) campaign from December 2015 to March 2016 allow an investigation of the influence of denitrification on the lowermost stratosphere (LMS) with a high spatial resolution. ~~For the first time~~ Two-dimensional vertical cross-sections of nitric acid (HNO_3) along the flight track and tracer-tracer correlations derived from the GLORIA observations document detailed pictures of wide-spread nitrification of the Arctic LMS during the course of an entire winter. GLORIA observations show large-scale structures and local fine structures with ~~strongly~~ enhanced absolute HNO_3 volume mixing ratios reaching up to 11 ppbv at altitudes of ~~11~~12 km in January and nitrified filaments persisting until the middle of March. Narrow ~~streaks~~ coherent structures tilted with altitude of enhanced HNO_3, observed in mid-January, are interpreted as regions recently nitrified by sublimating HNO_3-containing particles. ~~Overall, a~~ Overall, extensive nitrification of the LMS between 5.0 ppbv and 7.0 ppbv at potential temperature levels between 350 and 380 K is estimated. ~~This extent of nitrification has never been observed before in the Arctic lowermost stratosphere.~~ The GLORIA observations are compared with CLaMS (Chemical Lagrangian Model of the Stratosphere) simulations. The fundamental structures observed by GLORIA are well reproduced, but differences in the fine structures are diagnosed. Further, CLaMS predominantly underestimates the spatial extent of ~~maximum~~ HNO_3 ~~mixing ratios~~ maxima derived from the GLORIA observations as well as the ~~enhancement at lower altitudes~~overall nitrification of the LMS. Sensitivity simulations with CLaMS including (i) enhanced sedimentation rates in case of ice supersaturation (to resemble ice nucleation on NAT), (ii) a global temperature offset, (iii) modified growth rates (to resemble aspherical particles with larger surfaces) and (iv) temperature fluctuations (to resemble the impact of small-scale mountain waves) ~~mostly improve~~ slightly improved the agreement with the GLORIA observations ~~. The~~ of individual flights. However, no parameter could be isolated which resulted in a general improvement for all flights. Therefore, we conclude that a more comprehensive change in the model representations is required. Still, the sensitivity simulations suggest that details of particle microphysics play a significant role for simulated LMS nitrification

in January, while air subsidence, transport and mixing become increasingly important for the simulated HNO_3 distributions towards the end of the winter.

1 Introduction

The processes of denitrification and nitrification are well-known phenomena occurring in the polar winter stratosphere (Fahey et al., 1990). They involve the condensation, growth, sedimentation and sublimation of nitric acid (HNO_3)-containing polar stratospheric cloud (PSC) particles and result in an irreversible vertical redistribution of HNO_3. Denitrification is known to affect polar winter ozone loss (Fahey et al., 1990; Waibel, 1999). While denitrification at higher layers (i.e. around 16 to 22 km) attenuates fast deactivation of catalytically active chlorine species into the reservoir species chlorine nitrate ($ClONO_2$), chlorine deactivation can be fostered at lower layers enriched in HNO_3 (i.e. nitrified) by evaporating nitric acid trihydrate (NAT) particles (Fischer et al., 1997). Observational evidence for particles other than NAT involved in denitrification is sparse (e.g. Tabazadeh and Toon, 1996; Kim et al., 2006). Nitrification of the lowermost stratosphere is of particular interest since the chemical budget of reactive nitrogen (NO_y) and, thereby, its possible effects on ozone are modified in a region important for the radiative budget of the atmosphere (Riese et al., 2012).

While fundamental processes in connection with PSCs are well understood, there are still uncertainties concerning the formation of NAT particles and their characteristics that influence the processes of denitrification and nitrification. Chemistry-transport and global chemistry models including simplified microphysical properties of NAT are generally successful in simulating denitrification of the polar winter stratospheres (Carslaw, 2002; Grooß et al., 2005, 2014; Khosrawi et al., 2017; Zhu et al., 2017, and references therein). However, parametrizations resulting in agreement with observed size distributions of NAT particles, particularly extremely large NAT particles, and reproducing fine-structures of observed denitrification patterns remain an issue (e.g. Molleker et al., 2014; Woiwode et al., 2014).

Hemispheric differences in nitrification are observed due to different conditions in Antarctic and Arctic winter vortices. In the Antarctic, cold and stable vortices result in widespread PSC coverage and denitrification over wide vertical ranges. PSCs are observed less frequently in the Arctic, and the degree of denitrification varies from winter to winter (Santee et al., 1999; Pitts et al., 2018, and references therein). Increasing greenhouse gas emissions could lead to lower stratospheric temperatures (e.g. Rex et al., 2006) which likely cause stronger denitrification of the Arctic stratosphere.

Numerous studies addressed denitrification in Arctic winters, especially in cold winters, e.g. 1994/1995 (Waibel, 1999), 1999/2000 (Popp et al., 2001), 2004/2005 (Jin et al., 2006), 2009/2010 (Khosrawi et al., 2011; Woiwode et al., 2014), 2010/2011 (Sinnhuber et al., 2011) and 2015/2016 (Khosrawi et al., 2017). While most of these studies focused on the denitrification at altitudes higher than roughly 15 km, less attention was paid to the associated nitrification of lower layers. ~~Only~~ Dibb et al. (2006) reported nitrification at potential temperature levels above 340 K (around 12 km) at the end of January 2005. Further, Hübler et al. (1990) interpreted enhanced mixing ratios of up to 12 ppbv at altitudes between 10 and 12.5 km in the Arctic winter 1988/89 as resulting from nitrification. Tuck et al. (1997) found indications for nitrification in the Antarctic at levels above 400 K in the Antarctic winter 1994. Particularly, nitrification of the Arctic lowermost stratosphere (LMS) has

hardly been investigated. This is due to the fact that cold winters with strong denitrification were rare events in the Arctic stratosphere in the past and that the observational capabilities to resolve nitrification of the LMS with sufficient coverage and vertical resolution are sparse. For example, limb-sounders, like MLS (Microwave Limb Sounder; Waters et al., 2006) or MIPAS (Michelson Interferometer for Passive Atmospheric Sounding; Fischer et al., 2008) typically have vertical resolutions of around 3-5 km making it difficult to resolve fine-scale structures of NO_y redistribution.

The process of vertical HNO_3 redistribution is very sensitive to temperature. NAT particle nucleation can begin as soon as temperatures fall below NAT equilibrium temperature T_{NAT}. NAT particles are nucleated heterogeneously with low number densities on foreign nuclei such as meteoritic dust particles (Hoyle et al., 2013). Below T_{NAT}, these particle grow and sediment downward and they evaporate as temperatures rise above T_{NAT}. A simulation of this process is challenging as it depends both on the nucleation parametrisation and on the precise reproduction of the temperatures around T_{NAT}. This is especially the case during the onset of this process. At a later time, ~~the vertical HNO_3 redistribution may be saturated as due to the lower~~ in order to nucleate new NAT particles in denitrified air, lower temperatures are needed because of the already decreased HNO_3 mixing ~~ratio, no additional NAT particles can be nucleated.~~ ratios. This results in a maximum potential denitrification for a given temperature. Since both the nucleation process and the mesoscale temperature ~~is~~ modulations (e.g. by gravity waves) are not well known, it is especially difficult to simulate the small-scale structure of HNO_3 during the onset period.

Here, we present observations of nitrification of the LMS in the unusually cold Arctic winter 2015/2016 by the airborne limb-imaging Fourier transform infra red (FTIR) spectrometer GLORIA (Gimballed Limb Observer for Radiance Imaging of the Atmosphere, Friedl-Vallon et al. (2014); Riese et al. (2014)). In that winter, an extraordinarily cold and stable polar vortex (Matthias et al., 2016; Manney and Lawrence, 2016) promoted a long-lasting PSC phase from mid-December until the end of February with a large vertical extent (Pitts et al., 2018; Voigt et al., 2018) reaching down into the LMS.

Using the GLORIA observations, we investigate ~~the evolution of nitrification~~ following research questions:

- How are HNO_3 distributions structured in the LMS during the course of the ~~winter. Additionally, we~~ cold Arctic winter 2015/16? How do HNO_3 distributions, which are affected by nitrification, compare with the stratospheric tracer ozone? How do observed small-scale spatial patters compare with a model (CLaMS)?

- Do tracer-tracer correlations constructed from GLORIA HNO_3 and O_3 indicate nitrification of the LMS? How does nitrification inferred from the GLORIA observations compare with that inferred from CLaMS? Can we identify a critical model parameter which results in a significant overall improvement of the agreement?

Thereby, we attempt to quantify the observed nitrification, which is particularly difficult because the LMS composition is influenced by air masses originating from the Arctic vortex, the extra-vortex stratosphere and the troposphere (Werner et al., 2010; Gettelman et al., 2011; Krause et al., 2018). $ClONO_2$ also contributed significantly to lowermost stratospheric total NO_y during the Arctic winter 2015/16. This aspect is addressed within a separate study by Johansson et al. (2019). Here we focus only on gas-phase HNO_3, which is the direct product of nitrification by sublimating NAT particles.

~~Furthermore, we~~ We compare the GLORIA data with simulations by the Chemical Lagrangian Model of the Stratosphere (CLaMS; Grooß et al., 2014, references therein)~~and~~ . To test how well different parametrizations within the same model

reproduce the GLORIA observations~~.~~, four sensitivity studies were performed. Those sensitivity simulations investigated the impact of (i) enhanced sedimentation rates in case of ice supersaturation, (ii) a global temperature offset, (iii) modified growth rates and (iv) temperature fluctuations.

2 Aircraft Campaign and Data

2.1 POLSTRACC/GW-LCYCLE II/SALSA

The GLORIA observations analysed in this study were obtained during the combined POLSTRACC (POLar STRAtosphere in a Changing Climate), GW-LCYCLE II (Gravity Wave Life Cycle Experiment) and SALSA (Seasonality of Air mass transport and origin in the Lowermost Stratosphere using the HALO Aircraft) campaigns (PGS). Starting from Oberpfaffenhofen, Germany or Kiruna, Sweden 18 research flights were carried out by the German research aircraft HALO (High Altitude and LOng range research aircraft) between December 2015 and March 2016. The flights probed an entire winter period in the LMS at high northern latitudes. For this study five research flights between December and March were used. The selection of the flight data was based on data availability and scientific requirements. Data availability was limited to flight sections where GLORIA was operated in the high spectral resolution "chemistry mode" used in this study (see Sect. 2.2) and sufficiently cloud-free conditions allowing for the retrieval of HNO_3. From the scientific point of view, flights with long continuous "chemistry mode" measurements were chosen in order to show how patterns in the lowermost stratospheric HNO_3 distribution change during the winter. We furthermore focus on flights in January, where PSCs reached down to the LMS and where the most notable changes are found in the observed HNO_3 distributions. Since we use ozone as stratospheric tracer to quantify nitrification, flights in January are preferable since only little chemical ozone loss was diagnosed at this time of the winter when compared to February and March (see Johansson et al., 2019). Further GLORIA "chemistry mode" observations can be found in the supplementary information ofJohansson et al. (2018) and at the HALO Database (https://halo-db.pa.op.dlr.de/).

2.2 GLORIA

GLORIA is an airborne infrared limb imaging spectrometer (Friedl-Vallon et al., 2014). During PGS, GLORIA has been operated on board the HALO aircraft and pointed to the right hand side of the flight path. GLORIA combines a Michelson interferometer with an imaging HgCdTe detector which records 128 vertical and 48 horizontal interferograms simultaneously. All interferograms are transformed into spectra~~and~~. The spectra from horizontal detector rows are averaged for noise reduction prior to the atmospheric parameter retrieval (Kleinert et al., 2014). In high spectral resolution mode, which is used in this study, the spectrometer covers the range from 780 to 1400 cm^{-1} with a spectral sampling of 0.0625 cm^{-1}. For the retrieval, the radiative transfer code KOPRA (Karlsruhe Optimized and Precise Radiation transfer Algorithm; Stiller et al., 2002) and the inversion tool KOPRAFIT (Höpfner et al., 2001) were used. Estimated uncertainties of the GLORIA retrieval results are typically 1 - 2 K for temperature and 10 - 20% for trace gases. Typical vertical resolutions of the retrieved profiles are about

400 m at flight altitude and decrease to about 1000 m around the lowest tangent points. A detailed description and validation of the dataset used in this study is given by Johansson et al. (2018).

2.3 CLaMS

The Chemical Lagrangian Model of the Stratosphere (CLaMS) (McKenna, 2002a, b) is a chemistry transport model based on trajectory calculations for an ensemble of air parcels. CLaMS includes modules simulating Lagrangian trajectories, mixing, chemical processes and Lagrangian particle sedimentation. The CLaMS simulations used here were performed with a special setup for the POLSTRACC campaign with a horizontal resolution of about 100 km and a vertical resolution of about 500-900 m in the lower stratosphere above 10 km altitude decreasing to about 2 km below 9 km altitude. Further, this configuration includes a comprehensive stratospheric chemistry as described by Grooß et al. (2014). The simulations were performed for the entire winter and were based on meteorological wind and temperature data from the ECMWF ERA interim reanalysis (Dee et al., 2011) employing a horizontal resolution of 1x1 degrees and a timestep of 6 h. To simulate processes connected to NAT particles, particle parcels are implemented (Grooß et al., 2005, 2014). Particle size and number concentration are assigned to each particle parcel so that various particle parcels in one air parcel determine the particle size distribution. NAT and ice nucleation is temperature and saturation dependent and is parametrized by the scheme by Hoyle et al. (2013) and Engel et al. (2013), respectively. Particle growth and evaporation are calculated along particle trajectories based on Carslaw (2002) assuming the characteristics of spherical particles (Tritscher et al., 2019). Comparisons with PSC observations (Tritscher et al., 2018) show that the parametrisation of nucleation and sedimentation of NAT and ice particles in CLaMS is capable to reproduce the main features of PSC observations. Also, vortex averages of the vertical redistribution of HNO_3 and H_2O have been reproduced (Tritscher et al., 2019).

3 Methods

3.1 GLORIA vertical cross sections of atmospheric parameters

The GLORIA retrieval results in vertical ~~atmospheric parameter profiles~~ profiles of atmospheric parameters. These vertical profiles are combined to 2-dimensional quasi-vertical cross sections along the flight paths and show mesoscale atmospheric structures (Johansson et al., 2018). Since the observations are performed in limb-mode, the distance of the tangent points (i.e where the major information about atmospheric parameters stems from) gradually increases from the observer for the lower limb views. This is reflected by the tangent point distributions in Figs. ~~1a,~~ 2a, 3a and 4a. The GLORIA data is filtered for cloud-affected observations, and data points with a vertical resolution worse than 2 km or above flight altitude are neglected for further analysis.

3.2 Simulated cross sections from CLaMS

For comparison with GLORIA, the CLaMS data were interpolated to the retrieval grid geolocations, characterized by altitude, latitude, longitude and time of the tangent points. The temporal interpolation with respect to atmospheric dynamics is performed by trajectory calculations. CLaMS output is typically saved daily at 12:00 UTC. Therefore forward trajectories are calculated for points between 00:00 UTC and 12:00 UTC until 12:00 UTC. The corresponding 12:00 UTC volume mixing ratio is then assumed as concentration of the original geolocation based on the assumption that chemical and physical changes in volume mixing ratios during the time of the trajectory calculations are negligible for the chemical species considered here. For points between 12:00 UTC and 00:00 UTC backward trajectories are calculated analogously.

3.3 Identification of sub-vortex air

The altitude range of GLORIA observations in this study typically lies within the LMS, ranging from the tropopause to the 380 K isentrope (see Werner et al., 2010, and references therein). It has to be pointed out that robust identification of vortex air in the LMS is not possible due to dynamical disturbances, transport and in-mixing of air masses from different origins. In fact, the sub-vortex region in the LMS has a more filamentary character and is affected by interaction with air masses from the extra-vortex stratospheric overworld, the extra-tropical transition layer (ExTL), and the troposphere (Gettelman et al., 2011). Two filters have been applied in order to select data points associated with the sub-vortex region.

The first filter applied is the criterion by Nash et al. (1996) at the 370 K isentrope and based on the PV field obtained from the ~~Merra-2 reanalysis~~ MERRA-2 reanalysis (Gelaro et al., 2017). Grid points with latitude-longitude pairs outside the polar vortex at the potential temperature (θ) level of 370 K are classified as non-vortex points. Secondly, data is filtered by scaled potential vorticity (sPV) calculated from ~~Merra-2~~ MERRA-2 reanalysis data with a threshold of ~~$1.2 \cdot 10^{-4} s^{-1}$~~ $1.2 \times 10^{-4} s^{-1}$. sPV is calculated by dividing the potential vorticity (PV) by $\partial\theta/\partial p$ to obtain similar PV ranges for all isentropic levels that are investigated (Manney et al., 1994; Dunkerton and Delisi, 1986). Therefore this filter takes the altitude information of the grid points into account. Data points in the tracer correlations (see below) are attributed to sub-vortex air, if both criteria are met.

4 ~~GLORIA observations and CLaMS simulations of selected flights from January to March 2016~~

3.1 ~~Flight 6~~ Quantification of nitrification based on ~~12 January 2016~~tracer-tracer correlations using relative normalized frequency distributions

~~(a) Flight path and vortex filtering according to the Nash criterion at 370 K for flight 6 on 12 January 2016. White line: flight track with characteristic waypoints (A, B); light grey shading: areas that are not associated with the polar vortex. Cross-sections of (b) O_3 and (c) HNO_3 distribution derived from GLORIA and (d) HNO_3 distribution simulated by CLaMS for flight 6 on 12 January 2016. Flight altitude (bold black line), characteristic waypoints (A, B), 340 K and 370 K potential temperature levels (ECMWF, dashed black lines) and 2 PVU level (ECMWF, black line).~~

Flight 6 started on 12 January 2016 from Oberpfaffenhofen as the transfer flight to Kiruna. At the flight day, the identified vortex region(indicated by non-shaded areas in Fig. **??**a) appears relatively coherent by applying the Nash criterion at θ = 370 K. Only above the British Isles, southern Scandinavia and north-west of Norway patches of air masses do not fulfil this filter criterion. Further, PSCs were observed above flight altitude towards the end of the flight near Kiruna (Pitts et al., 2018).

Maximum ozone volume mixing ratios of 1.2 ppmv are observed between 11:40 and 12:10 UTC close to the flight altitude (Fig. **??**b) To quantify nitrification in the LMS tracer-tracer correlations of HNO_3 and O_3 associated with sub-vortex air are analysed. Here, we use ozone as an approximation of a passive reference tracer, since ozone is well accessible with GLORIA and shows a sufficient vertical gradient in the LMS region. Except for flight segments with a high tropopause (indicated by the The choice of ozone as a passive tracer is based on the assumption that ozone depletion is small in that period as the air is hardly exposed to sunlight. The model study by Khosrawi et al. (2017) supports this assumption. Two aspects can affect the correlation: 1) Mixing with extra-vortex air masses not affected by nitrification would lead to an underestimation of HNO_3 introduced into the LMS by nitrification and 2PVU level) from 09:00 to 11:20 UTC outside the vortex region, ozone volume mixing ratios of about 0.5 ppmv are observed around the 340 K isentrope. The) Potential ozone depletion would shift higher HNO_3 mixing ratios to lower ozone values, thus enhancing estimated nitrification.

As correlation scatter plots of measured data for several flights are difficult to assess due to the large number of individual points, estimates of relative normalized frequency distributions (RNFD) as described by Eckstein et al. (2018) are used in this study. This method calculates a scaled two dimensional histogram on a volume mixing ratio grid. In this study a grid of 0.070 ppmv O_3 $\times$ 0.35 ppbv HNO_3 volume mixing ratios (Fig. **??**c) show a more complex pattern. The structures until 11:is chosen, which is motivated by the total estimated error of the trace gases (Johansson et al., 2018). GLORIA data points with a calculated relative error larger than 20 UTC show a similar pattern as ozone, corresponding with the non vortex region. Further, maximum % are neglected in this study. Besides a clearer presentation of the data points, RNFDs filter out single data points with very high HNO_3 volume mixing ratioswell exceeding 8 ppbv are observed around 12:00 UTC close to flight altitude. While the ozone distribution after 12:00 UTC appears relatively coherent along an isentrope, values differ significantly for . Therefore, in the context of a challenging vortex identification this method offers an additional filter, as single data points that are differing significantly and are erroneously identified as vortex air are filtered out. Here it has to be pointed out that also local non-erroneous points with very high HNO_3 values within the vortex are filtered out applying this method. However, in this study we aim to quantify the overall nitrification of the LMS, while local nitrification is highly inhomogeneous and can reach significantly higher values. Here, maximum valuesspread over fewer data points . Moreover, a band-like structure of enhanced The RNFD contour line used for quantification in this study includes points within 2% of the histograms maximum density. An example of a RNFD for the HNO_3values appears between 12:00 and 13:00 UTC. In summary, -O_3-correlation during flight 8 is given in Figure 1.

4 GLORIA observations and CLaMS simulations of selected flights from January to March 2016

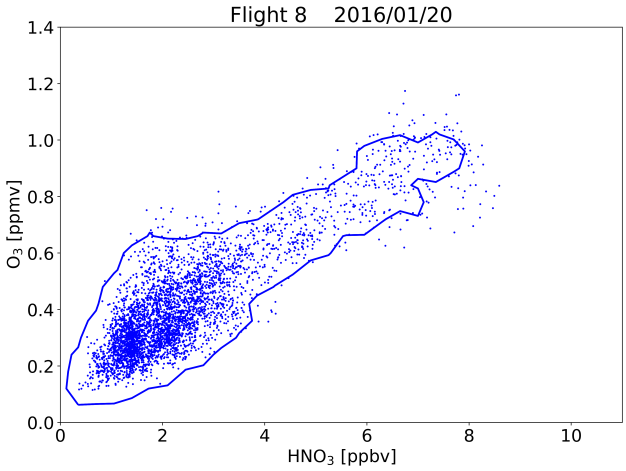

Figure 1. Correlation of HNO_3 with O_3 measured by GLORIA during flight 8 on 20 January 2016. The correlation is shown as single points and as RNFD (solid lines).

In order to investigate how the observed HNO_3 ~~structures exhibit a much larger spatial variability than those observed in the ozone distribution , indicating their formation due to redistribution processes.~~

~~The modelled HNO_3 volume mixing ratios (Fig. **??**d) show a maximum of 8 ppbv between 11:50 and 12:~~distribution is affected by nitrification, three research flights have been selected. The first flight was carried out on 20 ~~UTC at altitudes between 12 and 13 km, well matching the location where the maximum is observed by GLORIA. Further, CLaMS models slightly enhanced~~ January 2016 during the coldest phase of the winter (Manney and Lawrence, 2016), with PSCs ranging down to flight level. The second flight took place on 31 January 2016 after a strong PSC phase. The last flight was carried out on 18 March 2016 at a late state of the winter - about two weeks after the final warming (5-6 March; Manney and Lawrence, 2016).

The observed patterns in the HNO_3 ~~volume mixing ratios at flight altitude at 12:50 UTC corresponding to the maximum of the band-like structure observed by GLORIA. Compared to the observations, CLaMS shows a similar overall structure but is not able to reproduce the band-like structure. CLaMS underestimates the maximum~~ distributions are compared with the observed patterns in the ozone distribution. Since ozone and HNO_3 ~~volume mixing ratios for most flight segments and doesn't model an enhancement down to the same altitudes as observed by GLORIA. We point out that enhancements at low altitudes are potentially not well reproduced due to the model's low vertical resolution of about 2 km at altitudesbelow 9 km.~~ are effected by the same dynamical processes, the different patterns in the observed distributions are likely caused by processes that effect only one species (i.e. nitrification due to sublimation of NO_y-containing particles sedimented from higher altitudes). Therefore, the local HNO_3 enhancements seen in comparing adjacent air masses at a given height level and the deviations of their pattern from the pattern seen in the ozone distribution are interpreted qualitatively as a result of nitrification.

4.1 Flight 8 on 20 January 2016

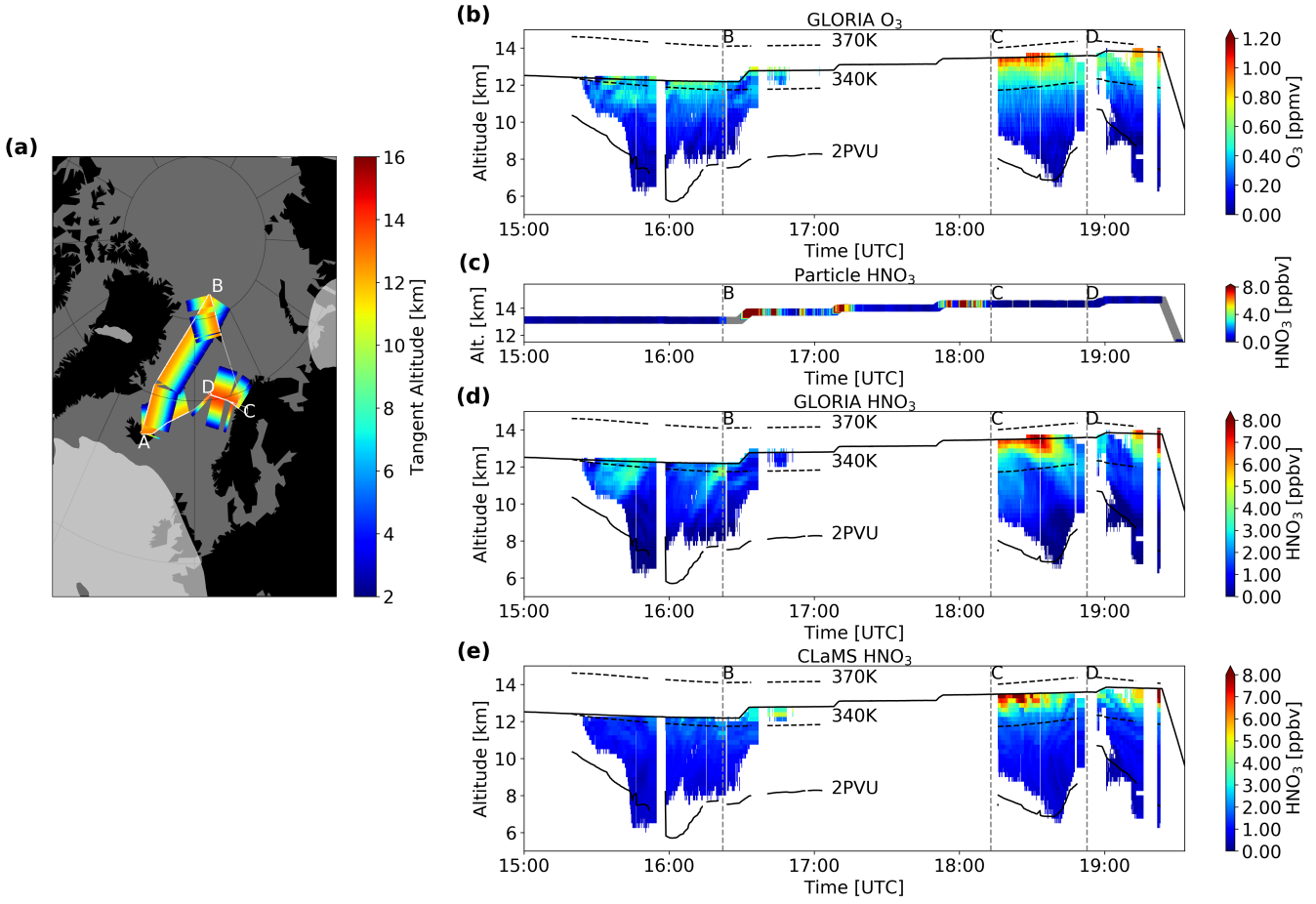

Figure 2. (a) Flight path and vortex filtering according to the Nash criterion at 370 K for flight 8 on 20 January 2016. White line: flight track with characteristic waypoints (A, B, C, D); ~~light~~ dark grey shading: areas that are ~~not~~ associated with the polar vortex. ~~Cross-sections of~~ (b) Cross-section of O_3 ~~and (d) HNO_3~~ distribution derived from GLORIA ~~and (e) HNO_3 distribution simulated by CLaMS~~ for flight 8 on 20 January 2016. Flight altitude (bold black line), characteristic waypoints (B, C, D), 340 K and 370 K potential temperature levels (~~ECMWF~~MERRA-2, dashed black lines) and 2 PVU level (~~ECMWF~~MERRA-2, black line). (c) Particulate nitrate measurements at flight altitude for flight 8 on 20 January 2016 (not enhancement corrected). (d) Cross-section of HNO_3 distribution derived from GLORIA and (e) HNO_3 distribution simulated by CLaMS for flight 8 on 20 January 2016. Flight altitude (bold black line), characteristic waypoints (B, C, D), 340 K and 370 K potential temperature levels (MERRA-2, dashed black lines) and 2 PVU level (MERRA-2, black line). The cross-sections and particulate nitrate measurements show only the flight part after waypoint A.

~~The flight on 20 January 2016 started and ended in Kiruna and took place during in the coldest phase of the winter (Manney and Lawrence, 2~~ ~~.~~ Applying the Nash criterion on 20 January 2016, a relatively coherent vortex region is found, with all GLORIA tangent points located inside the vortex region at θ = 370K (Fig. 2a). ~~The flight was carried out during particularly cold conditions, with PSCs ranging down to flight level.~~ Since clouds complicate a robust trace gas retrieval, a number of GLORIA observations

~~where sorted out~~ were removed by cloud-filtering. As a consequence, only limited GLORIA nitric acid data are available in flight sections with sufficiently transparent conditions (Fig. 2b). Further, particulate NO_y (i.e. the difference between measured total NO_y and gas-phase NO_y) was simultaneously measured in-situ by using a chemiluminescence-detector in combination with a converter for NO_y species (Stratmann et al., 2016). Similar observations have also been made during other aircraft campaigns in the Arctic (Northway et al., 2002). NO_y-containing particles were vaporized and detected as gas phase-equivalent total NO_y~~*~~. In Fig. 2c, we show the measurements taken during the flight on 20 January 2016 which are not corrected for enhancement efficiency (Ziereis et al., 2004). ~~We~~ As absolute values can not be obtained, we only use the data as a proxy for condensed ~~particulate~~ HNO_3-containing particles present at flight altitude. The in situ data clearly confirm the presence of HNO_3-containing PSC particles at flight altitude and in the vicinity of the local HNO_3 maxima detected by GLORIA.

The vertical cross-sections of O_3 and HNO_3 volume mixing ratios along the HALO flight track derived from GLORIA are depicted in Fig. 2b, d. The ozone distribution shows increasing volume mixing ratios with altitude reaching 1.1 ppmv at 13 km. The observed O_3 volume mixing ratios vary only moderately at fixed altitude levels during the whole flight in agreement with the location of the measurements within the vortex and the homogeneity inside the vortex. Compared to the ozone distribution, the HNO_3 volume mixing ratios are varying significantly at fixed altitudes. The HNO_3 distribution shows ~~enhanced~~ high HNO_3 volume mixing ratios particularly in the flight segment between the waypoints C and D, reaching up to 8 ppbv at a flight altitude of 13 km compared to 3 ppbv observed in adjacent air around waypoint D. ~~Enhanced values are forming band-like structures~~ Differences of this maximum structure from the corresponding O3 distribution are interpreted qualitatively as nitrified air. Further, local maxima are forming coherent structures tilted with altitude and are observed down to 11 km in that flight segment. ~~Further~~In addition, small scale fine structures with enhanced HNO_3 volume mixing ratios appear between 15:30 and 17:00 UTC and reach down to 10 km. The pattern of continuous and slightly tilted vertical bands differ significantly from the ozone distribution ~~, indicating~~ and show enhanced values compared to adjacent air masses at a given height level, thus suggesting their formation by redistribution of HNO_3. The simultaneous presence of confined local gas phase HNO_3 maxima in the GLORIA data and HNO_3-containing particles detected in situ in regions close to the equilibrium temperature of NAT and well above the equilibrium temperature of ice (see GLORIA temperature data shown in Johansson et al., 2018) suggests that an ongoing nitrification process was probed.

The vertical cross-section of HNO_3 volume mixing ratios modelled by CLaMS is shown in Fig. 2e. HNO_3 volume mixing ratios reach maximum values of 8 ppbv at flight altitude in the flight segment between C and D. While maximum HNO_3 volume mixing ratios in this flight are well represented by CLaMS, slight differences in the location of the maximum occur. ~~Enhanced~~ Overall HNO_3 ~~volume mixing ratios reach down to only 11 km compared to 9 km for the GLORIA observations. Additionally, CLaMSshows slightly enhanced HNO_3 volume mixing ratios around 16:00 UTC but does not represent the small scale fine structures observed between 15:30 and 17:00 UTC~~mixing ratios are clearly underestimated by CLaMS.

4.2 Flight 12 on 31 January 2016

At the end of January 2016, applying the Nash criterion at θ = 370K, a more disturbed lower vortex region is observed. As shown in Fig. 3a, a large region between Greenland, central Europe and northern Siberia fulfilled the vortex criterion. However,

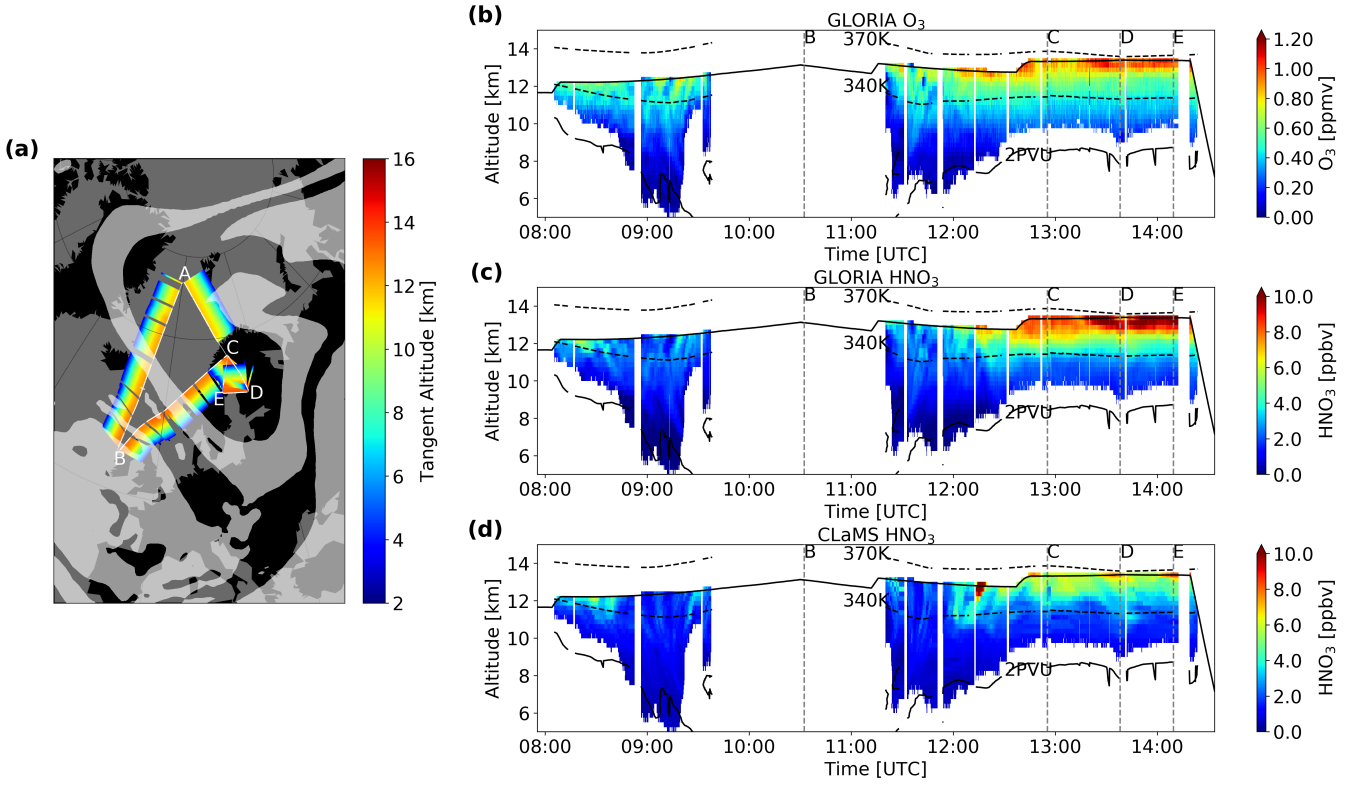

Figure 3. (a) Flight path and vortex filtering according to the Nash criterion at 370 K for flight 12 on 31 January 2016. White line: flight track with characteristic waypoints (A, B, C, D, E); ~~light~~ dark grey shading: areas that are ~~not~~ associated with the polar vortex. Cross-sections of (b) O_3 and (c) HNO_3 distribution derived from GLORIA and (d) HNO_3 distribution simulated by CLaMS for flight 12 on 31 January 2016. Flight altitude (bold black line), characteristic waypoints (B, C, D, E), 340 K and 370 K potential temperature levels (~~ECMWF~~MERRA-2, dashed black lines) and 2 PVU level (~~ECMWF~~MERRA-2, black line). The cross-sections show only the flight part after waypoint A. Please note the changed colorbar for HNO_3 compared to Figs. **??**,2,4.

filaments of lower PV are found from Greenland to southern Scandinavia and around the eastern rim of Scandinavia. Flight 12 was carried out starting and ending in Kiruna on 31 January and intersected several times with filaments outside the vortex.

Measured cross-sections of O_3 and HNO_3 volume mixing ratios are depicted in Fig. 3b and 3c. Except for the flight segments between 8:40 UTC and 9:20 UTC as well as 11:30 UTC and 11:50 UTC, that are associated with vortex edge or non vortex air, ozone values increasing with height are observed. ~~During this flight, enhanced~~ Compared to the ozone values only varying slightly along an isentrope, the HNO_3 volume mixing ratios ~~of up to 6 ppbv are measured around 8:15 UTC at flight altitude. Additionally, a pattern of strongly enhanced HNO_3 volume mixing ratios appears between 12:15 and 14:30 UTC at altitudes from 11 to 14 km, reaching~~ show larger variations at levels of constant potential temperature and suggest local enhancements by nitrification. During this flight, high local maximum values well above 10 ppbv are found between 13:30 UTC and 14:30 UTC

~~slightly below flight altitude. Since those structures between waypoints C and E vary significantly from those observed in the ozone concentrations they most likely originated from nitrification~~in the GLORIA observations.

The HNO_3 distribution modelled by CLaMS is shown in Fig. 3d. ~~Around 8:10 UTC enhanced HNO_3 volume mixing ratios of 6 ppbv are modelled. Further, enhanced~~ When compared to GLORIA, locally more confined and weaker HNO_3 ~~volume mixing ratios~~ maxima are modelled after 12:15 UTC reaching down to altitudes of 12 km~~, slightly higher in altitude than for the GLORIA observations~~. Maximum HNO_3 volume mixing ratios are found at flight altitude showing narrow peaks up to 10 ppbv at 12:15 UTC and 8 ppbv at 12:50 UTC, at waypoint D and E. Overall, CLaMS shows a higher spatial variability and underestimates the maximum values during large parts of the flight.

4.3 Flight 21 on 18 March 2016

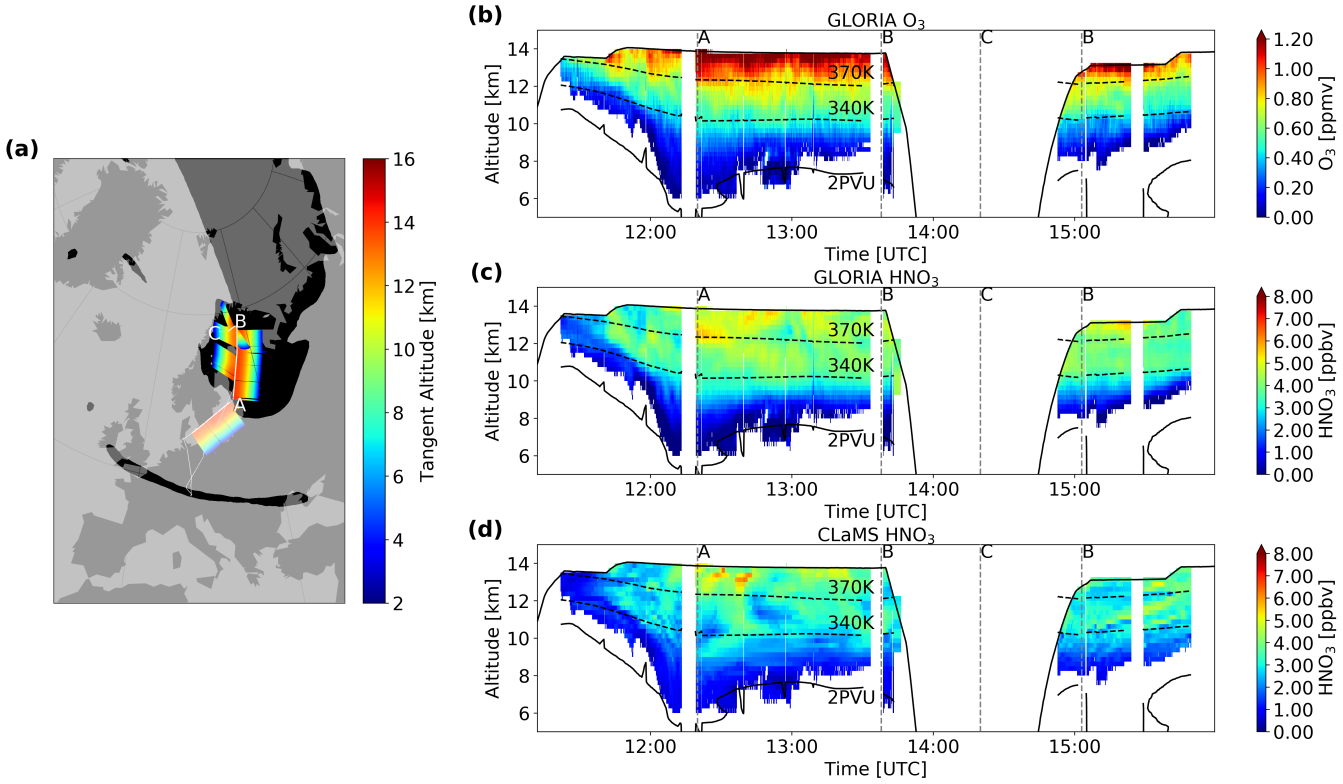

Figure 4. (a) Flight path and vortex filtering according to the Nash criterion at 370 K for flight 21 on 18 March 2016. White line: flight track with characteristic waypoints (A, B, C); ~~light~~ dark grey shading: areas that are ~~not~~ associated with the polar vortex. Cross-sections of (b) O_3 and (c) HNO_3 distribution derived from GLORIA and (d) HNO_3 distribution simulated by CLaMS for flight 21 on 18 March 2016. Flight altitude (bold black line), characteristic waypoints (A, B, C), 340 K and 370 K potential temperature levels (~~ECMWF~~MERRA-2, dashed black lines) and 2 PVU level (~~ECMWF~~MERRA-2, black line).

~~The~~ For the flight on 18 March 2016 ~~allowed further sampling of the vortex region at a late state of the winter - about two weeks after the final warming (5-6 March; Manney and Lawrence, 2016). The~~ the PV distribution shows a patchy pattern of regions inside the remains of the vortex according to Nash et al. (1996) around Scandinavia, with the GLORIA observations being located partly inside and outside these regions (Fig. 4a).

The measured O_3 distribution (Fig. 4b) shows increasing values with altitude and reaches values of 1.2 ppmv at flight level. Ozone values along the isentropes vary only slightly. The measured HNO_3 distribution (Fig. 4c) shows ~~enhanced values~~ a higher variability along the isentropes with local maxima for altitudes higher than 9 km reaching ~~maxima~~ maximum values of up to 6 ppbv at flight altitude embedded in background values of 2 to 3 ppbv. Filamentation and mixing following the earlier vortex break-up resulted in less spatial variability when compared to the previous flights. However, well-defined local ~~structures originating from nitrification~~ maxima qualitatively attributed to result from nitrification by the comparison with the ozone distribution still persisted in this late stage of the winter.

CLaMS (Fig.4d) shows ~~enhanced~~ HNO_3 volume mixing ratios for altitudes higher than 9 km corresponding well with GLORIA observations. Maximum values of locally 6 ppbv are modelled around 12:30 UTC at 13 km. ~~While maximum values are well represented, CLaMS generally underestimates the enhancements and shows a similar spatial variability~~ Again, CLaMS slightly underestimates overall HNO_3 mixing ratios when compared to GLORIA.

5 Quantification of nitrification of the LMS from December 2015 to January 2016

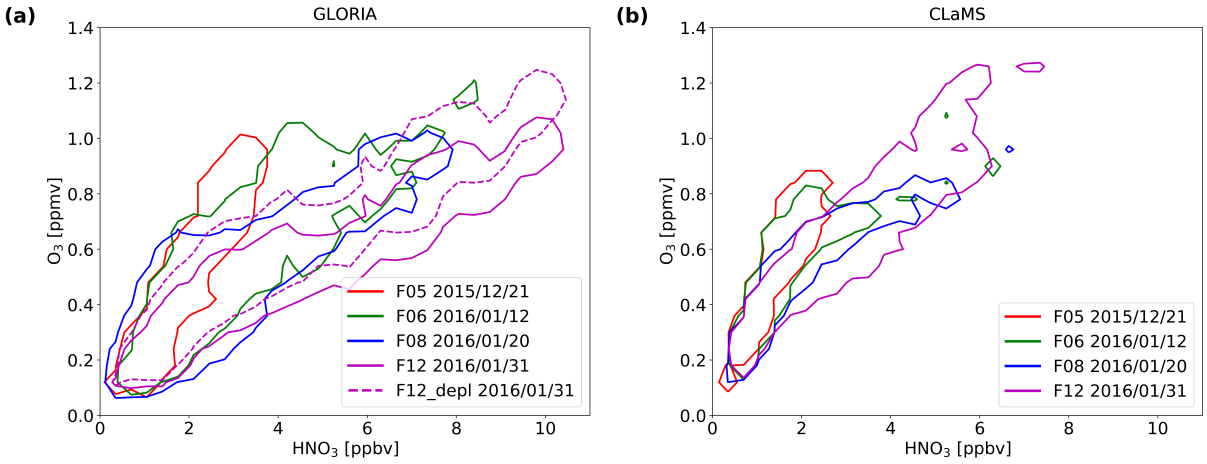

Figure 5. Isolines (contours at 0.02) of the normalized frequency distribution of the O_3-HNO_3-correlation for December 2015 - January 2016 derived from (a) GLORIA measurements and (b) CLaMS simulations. The dashed line for flight 12 includes a compensation of a potential ozone loss of 15 %.

To quantify nitrification in the LMS from December 2015 to January 2016 ~~HNO_3-O_3-correlations associated with sub-vortex air are analysed for selected flights in this period. GLORIA data points with a calculated relative error larger than 20% are~~

neglected in this study. Here, we use ozone as an approximation of a passive reference tracer, since ozone is well accessible with GLORIA and shows a sufficient vertical gradient in the LMS region. The choice of ozone as a passive tracer is based on the assumption that ozone depletion is small in that period as the air is hardly exposed to sunlight. The model study by Khosrawi et al. (2017) supports this assumption. Two aspects can affect the correlation: 1) Mixing with extra-vortex air masses not affected by nitrification would lead to an underestimation of HNO_3 introduced into the LMS by nitrification and 2) Potential ozone depletion would shift higher HNO_3 mixing ratios to lower ozone values, thus enhancing estimated nitrification.

As correlation scatter plots of measured data for several flights tend to be hard to assess due to the large number of individual points, estimates of relative normalized frequency distributions (RNFD) as described by Eckstein et al. (2018) are used in this study. This method calculates a scaled two dimensional histogram on a volume mixing ratio grid. In this study a grid of 0.070 ppmv O_3 × 0.35 ppbv HNO_3 is chosen, which is motivated by the total estimated error of the trace gases (Johansson et al., 2018). Besides a clearer presentation of the data points, RNFDs filter out single data points with very high HNO_3 volume mixing ratios. Therefore, in the context of a challenging vortex identification this method offers an additional filter, as single data points that are differing significantly and are erroneously identified as vortex air are filtered out. Here it has to be pointed out that also local non-erroneous points with very high HNO_3 values within the vortex are filtered out applying this method. However, in this study we aim to quantify the overall nitrification of the LMS, while local nitrification is highly inhomogeneous and can reach significantly higher values. The RNFD contour line used for quantification in the following section includes points within 2% of the histograms maximum density.

Isolines (contours at 0.02) of the normalized frequency distribution of the O_3-HNO_3-correlation for December 2015 – January 2016 derived from (a) GLORIA measurements and (b) CLaMS simulations.

we applied the method described in section 3.4 using selected flights in this period. Fig. 5a depicts the distributions for flights 5, 6, 8 and 12 derived from GLORIA observations. Flight 5 (not discussed here in detail since GLORIA observations are only available for a relatively short flight section without strong HNO_3 modulations for this flight) was carried out on 21 December 2015, at the beginning of the winter, with no significant hints to nitrification. Therefore this flight was chosen as early winter reference. Due to a limited number of points associated with vortex air, non vortex points are also considered here as well. Flight 06 (also not discussed here in detail) covered a broad range of latitudes in the sub-vortex region and below PSCs (Pitts et al., 2018).

HNO_3 volume mixing ratios for flight 5 (red) range from 0.25 ppbv to 1.5 ppbv for 0.1 ppmv ozone to 2.8 ppbv to range up to 3.2 ppbv for ozone values of 1 ppmv with an approximately linear relationship . Those valuesare to the observed ozone values. This profile is used as early winter reference. In case of flight 6 (green) enhanced HNO_3 volume mixing ratios up to 7.5 ppbv are observed for ozone values of 1 ppmv. Further a maximum of 8 ppbv is reached for O_3 values of 1.2 ppmv. In comparison to compared to flight 5 enhanced values of HNO_3 are observed for all ozone values. Flight 8 shows a similar enhancement throughout the whole range of ozone mixing ratios observed, reaching maximum . While the enhancement is similar to flight 6, minimum HNO_3 volume mixing ratios of 8 ppbv values for ozone values of 0.9 ppmv higher than 0.7 ppmv are higher than for the flights before. For flight 12, maximum the HNO_3 volume mixing ratios of 10 ppbv are observed for ozone values of 1 ppmvreach higher values than for the previous flights. Altogether, comparing maximum values with the

early winter reference, an ongoing nitrification is observed between December 2015 and January 2016 reaching up to 7 ppbv at ozone values of 1 ppmv and 5 ppbv at ozone values of 0.6 ppmv. ~~Johansson et al. (2019) determined~~

Johansson et al. (2019) estimated an ozone depletion by 0.15 ppmv at 380 K for ozone values around 1.15 ppmv by the end of January 2016. Assuming this potential ozone depletion of 15% ~~in~~ (dashed profile in Figure 5a) in the LMS during the given time frame, the estimated nitrification would reduce to ~~5.5~~6 ppbv at 1 ppmv O_3 and ~~4.0~~3.5 ppbv at ozone values of 0.6 ppmv. This is a lower limit estimation, especially considering the contrary effect by mixing of non-vortex air masses.

Correlation-based approaches are also suitable for model comparisons. The exact reproduction of complex fine structures by models cannot be expected because of uncertainties in measurements and the model. Differences in the meteorological fields used for modelling, especially the temperature, can result in differing local structures. Since the investigated flights probed a wide range of the subvortex region, the obtained correlations can be regarded as representative for the (Arctic) sub vortex and allow for a comparison between model and measurement. We point out that observed differences in RNFDs can be caused by an inaccurate representation of processes influencing both, HNO_3 as well as O_3 volume mixing ratios.

The distributions simulated by CLaMS are shown in Fig. 5b. For flight 5 the HNO_3 volume mixing ratios ~~between 0.5 and~~ range up to 2.5 ppbv ~~are observed with maximum ozone volume mixing ratios of 0.85 ppmv~~in an approximately linear relationship. Flight 6 shows enhanced HNO_3 volume mixing ratios ~~of up to 3.5 ppbv for O_3 values up to 0.8 ppmv and patches of further enhanced HNO_3 for ozone values between 0.8 ppmv and 1 ppmv~~that are significantly lower than for the GLORIA observations. CLaMS models a further enhancement for flight 8 ~~reaching up to 5.5 ppbv HNO_3 for ozone values of 0.8 ppmv with a patch reaching 6.5 ppbv at 0.9 ppmv O_3. Flight~~ with a small patch reaching the maximum values observed by GLORIA. Similar to the GLORIA measurements, flight 12 displays the highest HNO_3 volume mixing ratios of ~~about 6.5 ppbv for ozone values between 0.9 ppmv and 1.2 ppmv. One patch reaches 7 ppbv .~~

all flights. However, the maximum values observed by CLaMS are 2 ppbv lower. Beneath 0.3 ppmv O_3 hardly any enhancement is observed over the duration of the flights. Overall, CLaMS is able to reproduce the general enhancement of HNO_3 during the winter leading to a nitrification of up to 4 ppbv for ozone values of 0.8 to 1 ppmv, which is by 3 ppbv HNO_3 lower than the GLORIA observations.

6 Comparison of GLORIA results with CLaMS sensitivity simulations

Four sensitivity simulations have been performed in order to investigate processes and aspects that have not been represented in the model so far. These sensitivity simulations were performed based on assumptions concerning particle formation and shape. Besides the formation of NAT on ice particles, ice can possibly accumulate on NAT particles (Voigt et al., 2018) resulting in larger particles with an enhanced settling velocity. Therefore in the ~~'ice settling' simulation a~~ 'ice settling' simulation the computed ice settling velocity (computed as described by Tritscher et al., 2019) was increased by a factor of 1.5 ~~times enhanced settling velocity is applied if~~ at all locations where the saturation ratio of ice, S_{Ice}, is larger than 1.2. Since NAT formation is temperature dependent a sensitivity simulation is performed with a global temperature offset of 1 K. Particle growth in CLaMS is based on the assumption of growth rates of spherical particles. However, Woiwode et al. (2016) found

indications for highly aspherical particles with an enhanced surface compared to spherical particles of the same volume. Since the HNO_3 uptake depends on the surface, a faster particle growth would occur. A 1.5 times enhanced particle growth was implemented in the 'aspherical particle' simulation. Changes in settling velocities due to different shapes have not been taken into account here. Several studies suggest a connection between orographically induced gravity waves and NAT formation (Davies et al., 2005; Carslaw et al., 1998; Höpfner et al., 2006). However small scale temperature fluctuations are not resolved by ERA interim temperatures. Therefore, artificial fluctuations according to (Tritscher et al., 2019) have been added in the 'temperature fluctuations' simulation.

The comparison is based on the RNFDs depicted for the individual flights in Fig. 6. ~~As an example, the cross-sections of the different simulations (Fig. A1) for flight 6 have been analysed as well.~~ The cross-sections for flights 6, 8, 12 and 21 can be found in the appendix (Fig. A1 A2, A3, A4).

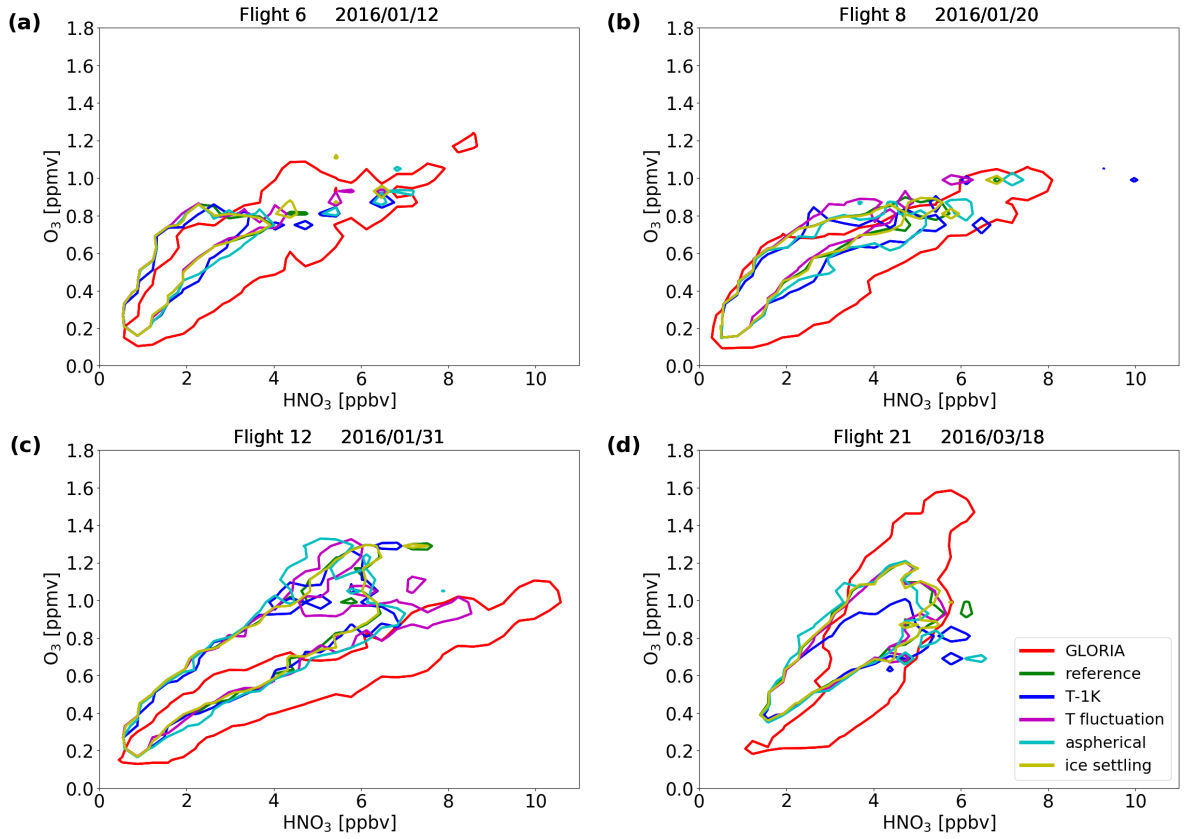

Figure 6. Isolines (contours at 0.02) of the normalized frequency distribution of the O_3-HNO_3-correlation for (a) flight 6 on 12 January 2016, (b) flight 8 on 20 January 2016, (c) flight 12 on 31 January 2016, (d) flight 21 on 18 March 2016 derived from GLORIA measurements (red) and CLaMS simulations.

6.1 ~~Flight 6 on 12 January 2016~~

~~Cross-sections of HNO_3 volume mixing ratio distribution for flight 6 on 12 January 2016 derived by GLORIA (a) and modelled by the CLaMS reference simulation (b) and sensitivity simulations considering (c) ice formation on NAT particles, (d) temperature fluctuations, (e) growth rates of aspherical particles, (f) 1K global temperature offset. Flight altitude (bold black line), characteristic waypoints (A, B, C), 340 K and 370 K potential temperature levels (ECMWF, dashed black lines) and 2 PVU level (ECMWF, black line).~~

The ~~sensitivity simulations'cross-sections for flight 6 are shown in Fig. A1c-f together with the GLORIA measurement in Fig. A1a and the reference simulation in Fig. A1b. The '~~'ice settling' simulation (~~Fig. A1c) delivers virtually~~ yellow) delivers nearly identical results as the reference simulation for ~~this flight. This is also observed in the RNFD depicted in Fig. 6a. The 'aspherical particle' case (Fig. A1e) shows a strengthening of existing maxima. The RNFD supports this observation and shows enhanced values down to lower altitudes than the reference simulation. Further, the band like structure observed by GLORIA around 12:40 UTC is more pronounced in the cross-section of this simulation. The absolute values there are still underestimated. The '~~all flights. For the 'T-1K' simulation (~~Fig. A1f)shows a maximized area of enhanced values that are reaching further down. This enhancement at lower altitudes also appears in the RNFD. Moreover, the band-like structure around 12:40 UTC is more developed than in the reference simulation. For the 'temperature fluctuation' simulation (Fig. A1d) slightly lower enhancements are found. However, the overall structure in the RNFD is similar to the reference simulation.~~

6.1 ~~Flight 8 on 20 January 2016~~

~~For flight 8, relative normalized frequency distributions are shown in Fig. 6b for all CLaMS simulations together with the GLORIA result. The 'ice settling' simulation simulates nearly identical structures as the reference simulation. For 'T-1K',~~ dark blue), enhanced HNO_3 volume mixing ratios are observed down to lower O_3 volume mixing ratios compared to the reference ~~simulation~~simulations for flight 6 and 8, but are still not reaching down to the ozone values noticed by GLORIA. The ~~RNFD for this simulation shows best agreement with the GLORIA observations. High~~ high HNO_3 volume mixing ratios measured by GLORIA are still underestimated here. While there are only slight changes compared to the reference simulation for flight 12, the 'T-1K' simulation is clearly deteriorating for flight 21. Here, lower ozone volume mixing ratios are observed. For this flight none of the CLaMS simulations is able to reproduce the high ozone volume mixing ratios observed by GLORIA, which is possibly caused by weaker subsidence in the model. Further, lower absolute HNO_3 values might occur due to stronger mixing in CLaMS. The 'aspherical particle' ~~simulation~~ case results in enhanced values observed down to lower altitudes than for the reference simulation ~~. The RNFD results in higher~~ for the flights 6, 8 and 12. Further, it shows higher maximum HNO_3 values ~~compared to the reference . However, there are also~~ than for the reference for flights 6 and 8. However, the absolute values are still underestimated compared to the GLORIA observations. For the flights 12 and 21 indications for points with lower ~~values than for the reference . For the~~ HNO_3 values compared to the reference are found. The RNFD structure of 'temperature fluctuation' ~~case lower HNO_3 volume mixing ratios are observed.~~

6.1 ~~Flight 12 on 31 January 2016~~

~~RNFDs for all sensitivity simulations are shown in Fig. 6c. The 'ice settling' case for flight 12 shows virtually identical results as~~ simulation for flight 6 and 21 are nearly identical to the reference simulation. For ~~the 'temperature offset' simulation higher maximum values are modelled at O~~flight 8, lower HNO_3 ~~volume mixing ratios between 600 and 900 ppbv. However, there are indications for lower~~ volume mixing ratios ~~for some points as well. For~~ are observed. In contrast to that, the 'temperature fluctuation' simulation ~~, a significant enhancement of maximum HNO_3 values is found reaching maximum values of 8 ppbv for ozone volume mixing ratios of 900 ppbv. This RNFD shows the~~ for flight 12 shows best agreement with the ~~GLORIA observationsfor this flight~~observations. However, even though the lower branch is consistent with GLORIA, an upper branch with values lower than the reference simulation and far lower than GLORIA exists. ~~The 'aspherical particle' simulation shows a distribution with higher spread and values partly higher, partly lower, than for the reference case.~~

6.1 ~~Flight 21 on 18 March 2016~~

~~For flight 21 the RNFDs are depicted in Fig. 6d. The 'ice settling' simulation, as well as the 'temperature fluctuation' simulation, shows only small differences compared to the reference simulation. In the 'aspherical particle' simulation enhanced values appear at slightly lower O_3 volume mixing rations than for the reference simulation. There are also indications for points with lower HNO_3 values. Generally, the different CLaMS simulations are similar in their structure, but the simulations differ significantly from the GLORIA results. The only simulation clearly deteriorating is the 'T-1K' case. For this flight none of the CLaMS simulations is able to reproduce the high ozone volume mixing ratios observed by GLORIA, which is possibly caused by weaker subsidence in the model. Further, lower absolute HNO_3 values might occur due to stronger mixing in CLaMS.~~

7 Discussion and Conclusion

Nitrification of the LMS in the Arctic winter 2015/16 was analysed based on GLORIA measurements during the PGS campaign. Vertical cross sections of HNO_3 volume mixing ratios for several flights throughout the winter show complex fine scale structures and enhanced values at altitudes down to 9 km. ~~For flight 6 in mid-January single profiles with HNO_3 volume mixing ratios exceeding 8 ppbv were observed.~~ Flight 8 on 20 January 2016 was carried out under cold conditions with PSC observations at flight altitude. For this flight, ~~band-like structures of~~ coherent structures tilted with altitude of locally enhanced HNO_3 volume mixing ratios are observed that most likely indicate defined regions where settled HNO_3-containing particles recently sublimated. This is supported by simultaneous in situ observations of HNO_3-containing particles. The net effect of proceeding nitrification and dynamical processes in the LMS is observed for flight 12 at the end of January with a pronounced pattern of enhanced HNO_3 volume mixing ratios well exceeding 10 ppbv. Nitrified filaments with HNO_3 volume mixing ratios up to 6 ppbv persist until flight 21 in March 2016. While cross-sections provide ~~an insight on the local nitrifications spatial and structural influence~~ a qualitative insight on local nitrification patters for selected flights, the extent of overall nitrification has been quantified based on HNO_3-O_3-correlations. Nitrification reached an extent of up to 7 ppbv at ozone values of 1 ppmv

($\theta \approx 370$ K) and up to 5 ppbv at ozone values of 0.6 ppmv ($\theta \approx 350$ K). A conservative correction, assuming a 15 % ozone loss on the correlations would reduce these numbers to ~~5.5~~6 ppbv and ~~4~~3.5 ppbv, respectively.

The comparison of GLORIA observations with the chemistry transport model CLaMS confirm the model's ability to reproduce nitrification of the LMS. Large-scale structures are reproduced by the model that also resolves complex fine structures, although differing from measured patterns. CLaMS predominantly underestimates the enhanced values observed by GLORIA. ~~Strongly enhanced~~ Enhanced values are found less frequently in the simulation and are limited to narrow regions. Further, modelled HNO_3 enhancements reach less far down on 12 and 20 January 2016 when compared with GLORIA. The CLaMS simulations result in a weaker nitrification of up to 4 ppbv for the period of December to January for ozone mixing ratios between 0.8 ppmv to 1 ppmv, which is by $\sim$3 ppbv lower than observed by GLORIA. For flight 21 in March, CLaMS underestimates the observed ozone volume mixing ratios, potentially indicating insufficient subsidence and stronger mixing in the model (Johansson et al., 2019). Sensitivity studies with CLaMS considering i) ice formation on NAT particles, ii) a 1 K global temperature offset, iii) growth rates of aspherical particles or iv) temperature fluctuations were performed. While the 'ice formation' simulation shows only slight differences, the other cases show ~~distinct differences for selected~~ noticeable differences during individual flights. The 'temperature fluctuation' simulation provides improved agreement for the flight on 31 January 2016, but also worsens the results for the flight on 20 January 2016. The 'T-1K' simulation improves the results for ~~all flights~~ the flights 6 and 8 in January, but deteriorates the results for the flight in the late winter on 18 March 2016. This shows the sensitivity of the simulation results on temperature. Potentially, a higher resolution in time and space would result in more realistic temperature fluctuations and could improve the simulations. The 'aspherical particle' case shows slightly more pronounced improvements for the flights in mid-January. Even though the sensitivity simulations ~~generally~~ partially improve the results, ~~significant~~ distinct differences between model and measurements remain. The sensitivity simulations suggest that particle microphysics play a significant role for LMS nitrification in January. Increasing discrepancies from the observations towards the end of the winter are attributed to simulated air subsidence, transport and mixing processes.

Several studies investigated nitrification in previous cold winters, although mainly with a focus on higher altitudes. Hübler et al. (1990) interpreted enhanced NO_y values of up to 12 ppbv at altitudes between 10 and 12.5 km in the Arctic winter 1988/89 as a result of nitrification. For the Arctic winter 2002/03 Grooß et al. (2005) modelled a nitrification of less than 1 ppbv for potential temperatures lower than 360 K. For the Arctic winter 2004/05, Dibb et al. (2006) observe nitrification of up to 3 ppbv for potential temperatures between 360 and 340 K. Jin et al. (2006) report an average nitrification of less than 2 ppbv for potential temperatures lower than 370 K for the same winter. Further, during the Arctic winter 2009/10 (Grooß et al., 2014) modelled a nitrification of less than 1 ppbv for potential temperatures lower than 360 K, while (Woiwode et al., 2014) found no significant indications for nitrification below 370 K. Since Arctic winters might show a tendency towards colder stratospheric temperatures (Rex et al., 2006), disturbances of the LMS NO_y budget by nitrification are likely becoming more frequent. During the Arctic winter 2015/16 exceptionally low stratospheric temperatures occurred and the vortex was sufficiently stable to allow formation of PSCs down to lowest stratospheric altitudes. Those conditions were the prerequisites for the strong nitrification observed and presented here. The measurements obtained by GLORIA during the POLSTRACC campaign document in detail a strong impact of nitrification on the LMS during an entire Arctic winter~~for the first time~~.

Data availability. The discussed GLORIA data set is available at the HALO database at https://halo-db.pa.op.dlr.de/ and at the KITopen repository (https://doi.org/10.5445/IR/1000086506). NASA MERRA-2 reanalysis data is available at https://disc.gsfc.nasa.gov/.

Appendix A

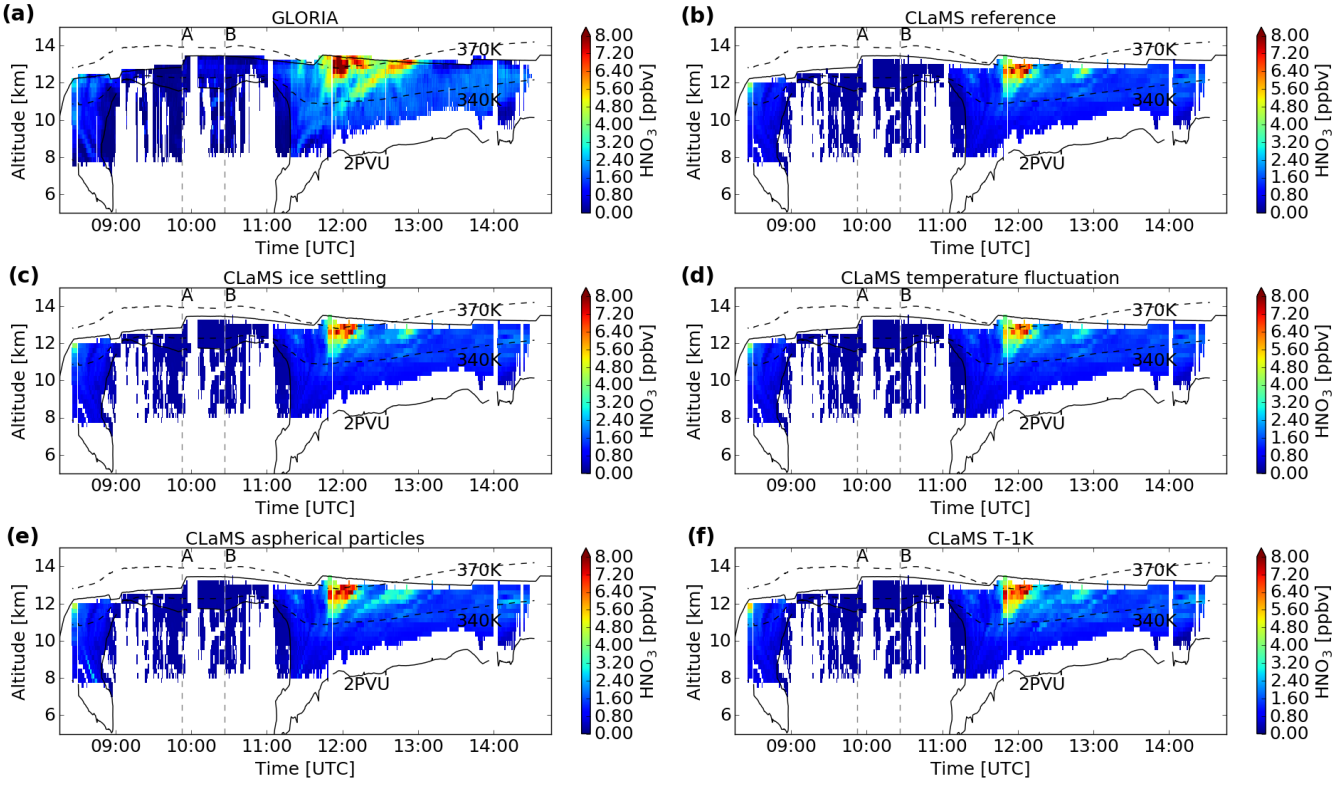

Figure A1. Cross-sections of HNO_3 volume mixing ratio distribution for flight 6 on 12 January 2016 derived by GLORIA (a) and modelled by the CLaMS reference simulation (b) and sensitivity simulations considering (c) ice formation on NAT particles, (d) temperature fluctuations, (e) growth rates of aspherical particles, (f) 1K global temperature offset. Flight altitude (bold black line), characteristic waypoints (A, B, C), 340 K and 370 K potential temperature levels (MERRA-2, dashed black lines) and 2 PVU level (MERRA-2, black line).

Author contributions. MB conducted the analysis and interpretation of GLORIA level-2 data and model simulations and prepared the manuscript with contributions from all co-authors. JUG performed the CLaMS model simulations. SJ, JU, WW performed the level-1 and -2 analysis of GLORIA data. MH contributed to the GLORIA data analysis and interpretation. FFV, PP operated the GLORIA instrument during the PGS campaign. HO, BMS coordinated the PGS field campaign. HZ provided the particle HNO_3 data. PB contributed to the interpretation and the manuscript preparation.

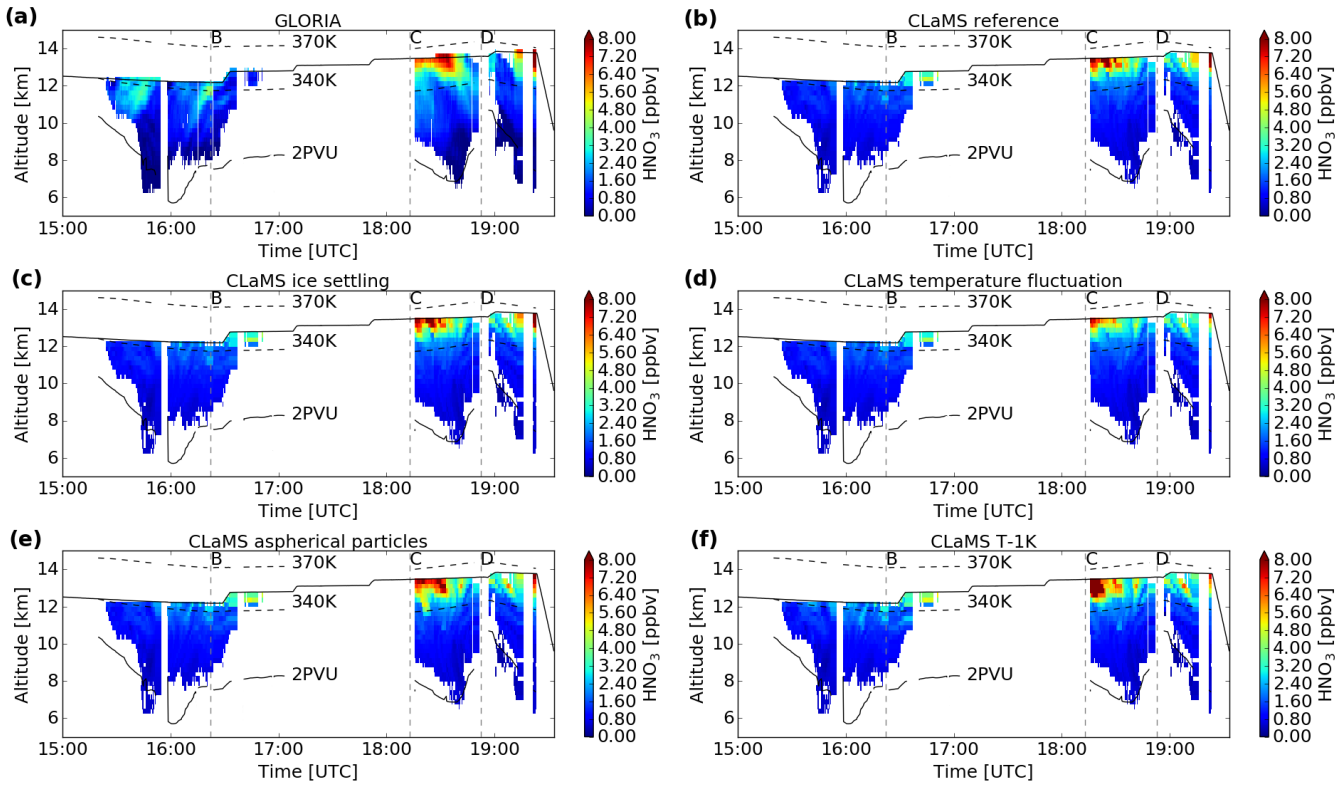

Figure A2. Cross-sections of HNO_3 volume mixing ratio distribution for flight 8 on 20 January 2016 derived by GLORIA (a) and modelled by the CLaMS reference simulation (b) and sensitivity simulations considering (c) ice formation on NAT particles, (d) temperature fluctuations, (e) growth rates of aspherical particles, (f) 1K global temperature offset. Flight altitude (bold black line), characteristic waypoints (), 340 K and 370 K potential temperature levels (~~ECMWF~~MERRA-2, dashed black lines) and 2 PVU level (~~ECMWF~~MERRA-2, black line).

Competing interests. The authors declare that they have no conflict of interest.

Acknowledgements. We thank the PGS coordination team and the DLR-FX for successfully conducting the field campaign. The results are based on the efforts of all members of the GLORIA team, including the technology institutes ZEA-1 and ZEA-2 at Forschungszentrum Jülich. We thank NASA for providing their ~~MERRA2~~ MERRA-2 meteorological reanalysis data set. We acknowledge the computing time for the CLaMS 5 simulations granted on the supercomputer JURECA at Jülich Supercomputing Centre (JSC) under the VSR project ID JICG11. This work was supported by the German Research Foundation (Deutsche Forschungsgemeinschaft, DFG Priority Program SPP 1294). S. Johansson has received funding from the European Community's Seventh Framework Programme (FP7/2007-2013) under grant agreement 603557. Further support was received by the German research initiative ROMIC (Role of the Middle Atmosphere in Climate) and by the German Ministry of Research and Education (BMBF) project "Investigation of the life cycle of gravity waves" (GW-LCYCLE, subproject

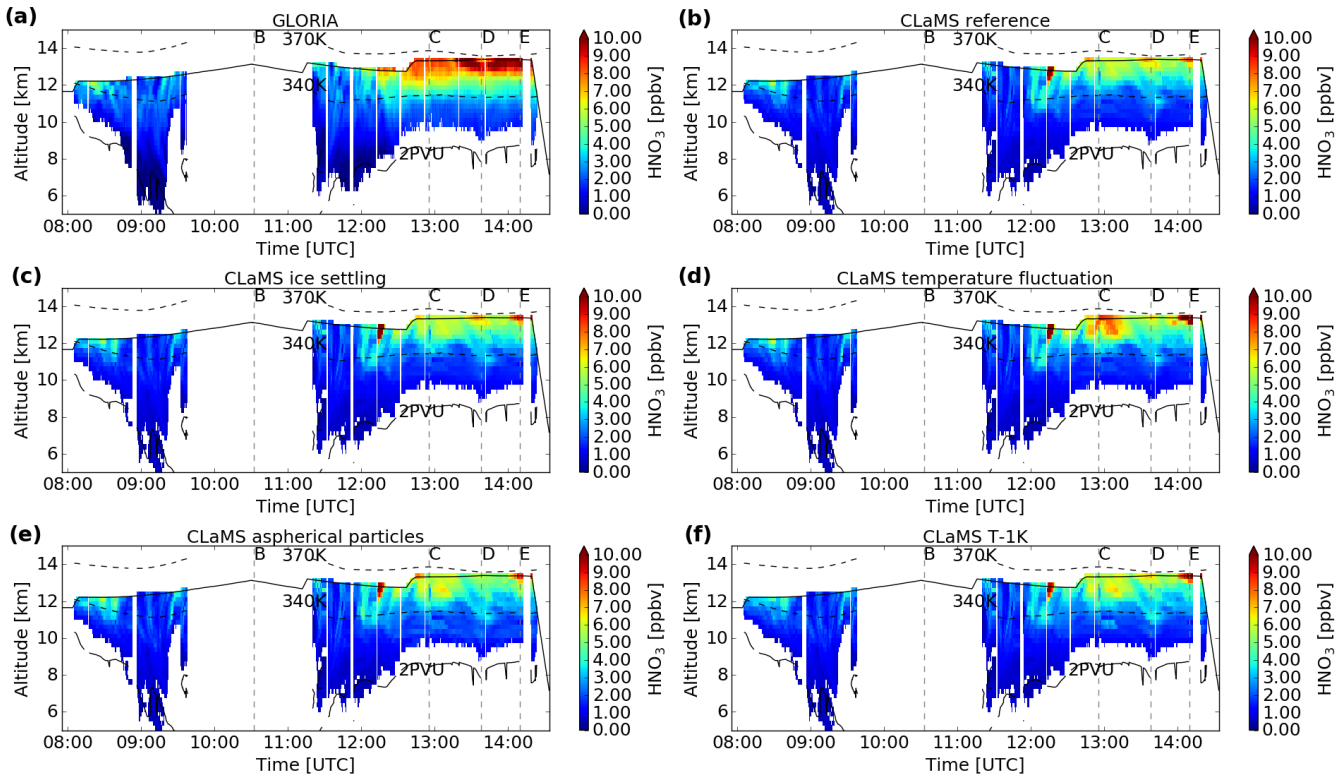

Figure A3. Cross-sections of HNO_3 volume mixing ratio distribution for flight 12 on 31 January 2016 derived by GLORIA (a) and modelled by the CLaMS reference simulation (b) and sensitivity simulations considering (c) ice formation on NAT particles, (d) temperature fluctuations, (e) growth rates of aspherical particles, (f) 1K global temperature offset. Flight altitude (bold black line), characteristic waypoints (), 340 K and 370 K potential temperature levels (~~ECMWF~~MERRA-2, dashed black lines) and 2 PVU level (~~ECMWF~~MERRA-2, black line). Please note the changed colorbar compared to Figs. A1,A2,A4.

2, 01LG1206B). We acknowledge support by the Deutsche Forschungsgemeinschaft and the Open Access Publishing Fund of the Karlsruhe Institute of Technology.

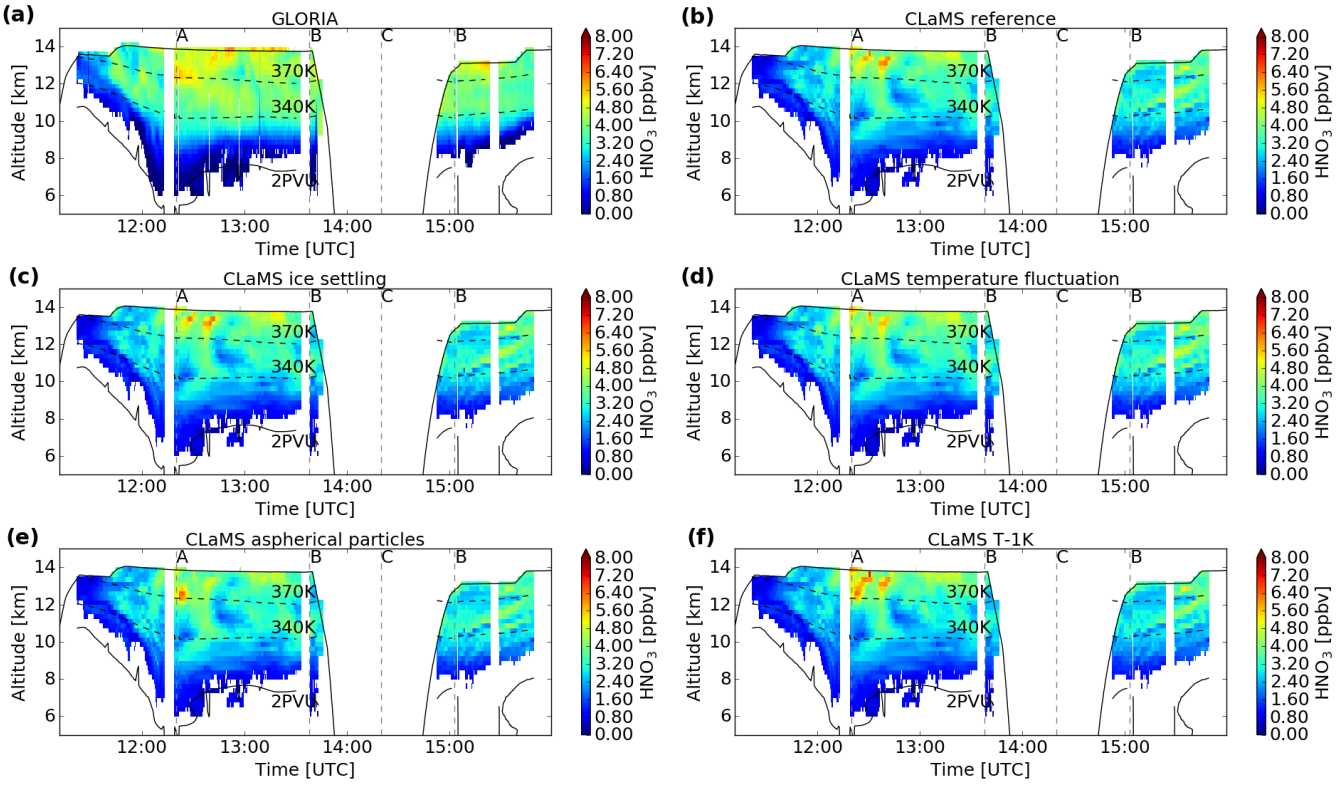

Figure A4. Cross-sections of HNO_3 volume mixing ratio distribution for flight 21 on 18 March 2016 derived by GLORIA (a) and modelled by the CLaMS reference simulation (b) and sensitivity simulations considering (c) ice formation on NAT particles, (d) temperature fluctuations, (e) growth rates of aspherical particles, (f) 1K global temperature offset. Flight altitude (bold black line), characteristic waypoints (A, B, C), 340 K and 370 K potential temperature levels (~~ECMWF~~MERRA-2, dashed black lines) and 2 PVU level (~~ECMWF~~MERRA-2, black line).

References

Carslaw, K. S.: A vortex-scale simulation of the growth and sedimentation of large nitric acid hydrate particles, Journal of Geophysical Research, 107, https://doi.org/10.1029/2001JD000467, 2002.

Carslaw, K. S., Wirth, M., Tsias, A., Luo, B. P., Dörnbrack, A., Leutbecher, M., Volkert, H., Renger, W., Bacmeister, J. T., and Peter, T.: Particle microphysics and chemistry in remotely observed mountain polar stratospheric clouds, Journal of Geophysical Research: Atmospheres, 103, 5785–5796, https://doi.org/10.1029/97JD03626, 1998.

Davies, S., Mann, G. W., Carslaw, K. S., Chipperfield, M. P., Kettleborough, J. A., Santee, M. L., Oelhaf, H., Wetzel, G., Sasano, Y., and Sugita, T.: 3-D microphysical model studies of Arctic denitrification: Comparison with observations, Atmospheric Chemistry and Physics, 5, 3093–3109, https://doi.org/10.5194/acp-5-3093-2005, 2005.

Dee, D. P., Uppala, S. M., Simmons, A. J., Berrisford, P., Poli, P., Kobayashi, S., Andrae, U., Balmaseda, M. A., Balsamo, G., Bauer, P., Bechtold, P., Beljaars, A. C. M., van de Berg, L., Bidlot, J., Bormann, N., Delsol, C., Dragani, R., Fuentes, M., Geer, A. J., Haimberger, L., Healy, S. B., Hersbach, H., Hólm, E. V., Isaksen, L., Kållberg, P., Köhler, M., Matricardi, M., McNally, A. P., Monge-Sanz,

B. M., Morcrette, J.-J., Park, B.-K., Peubey, C., de Rosnay, P., Tavolato, C., Thépaut, J.-N., and Vitart, F.: The ERA-Interim reanalysis: configuration and performance of the data assimilation system, Quarterly Journal of the Royal Meteorological Society, 137, 553–597, https://doi.org/10.1002/qj.828, https://rmets.onlinelibrary.wiley.com/doi/abs/10.1002/qj.828, 2011.

Dibb, J. E., Scheuer, E., Avery, M., Plant, J., and Sachse, G.: In situ evidence for renitrification in the Arctic lower stratosphere during the polar aura validation experiment (PAVE), Geophysical Research Letters, 33, https://doi.org/10.1029/2006GL026243, https://agupubs.onlinelibrary.wiley.com/doi/abs/10.1029/2006GL026243, 2006.

Dunkerton, T. J. and Delisi, D. P.: Evolution of potential vorticity in the winter stratosphere of January-February 1979, Journal of Geophysical Research, 91, 1199, https://doi.org/10.1029/JD091iD01p01199, 1986.

Eckstein, J., Ruhnke, R., Pfahl, S., Christner, E., Diekmann, C., Dyroff, C., Reinert, D., Rieger, D., Schneider, M., ~~Schröter~~Schröter, J., Zahn, A., and Braesicke, P.: From climatological to ~~small scale applications: Simulating~~ small-scale applications: simulating water isotopologues with ICON-ART-Iso (version ~~2.1),~~ 2.3), Geoscientific Model Development~~Discussions, accepted for GMD, pp. 1–31, , 2017.~~, 11, 5113–5133, https://doi.org/10.5194/gmd-11-5113-2018, https://www.geosci-model-dev.net/11/5113/2018/, 2018.

Engel, I., Luo, B. P., Pitts, M. C., Poole, L. R., Hoyle, C. R., Grooß, J.-U., Dörnbrack, A., and Peter, T.: Heterogeneous formation of polar stratospheric clouds – Part 2: Nucleation of ice on synoptic scales, Atmospheric Chemistry and Physics, 13, 10 769–10 785, https://doi.org/10.5194/acp-13-10769-2013, https://www.atmos-chem-phys.net/13/10769/2013/, 2013.

Fahey, D. W., Kelly, K. K., Kawa, S. R., Tuck, A. F., Loewenstein, M., Chan, K. R., and Heidt, L. E.: Observations of denitrification and dehydration in the winter polar stratospheres, Nature, 344, 321– 324, https://doi.org/http://dx.doi.org/10.1038/344321a0, 1990.

Fischer, H., Waibel, A. E., Welling, M., Wienhold, F. G., Zenker, T., Crutzen, P. J., Arnold, F., Bürger, V., Schneider, J., Bregman, A., Lelieveld, J., and Siegmund, P. C.: Observations of high concentrations of total reactive nitrogen (NO y) and nitric acid (HNO3) in the lower Arctic stratosphere during the Stratosphere-Troposphere Experiment by Aircraft Measurements (STREAM) II campaign in February 1995, Journal of Geophysical Research: Atmospheres, 102, 23 559–23 571, https://doi.org/10.1029/97JD02012, https://agupubs.onlinelibrary.wiley.com/doi/abs/10.1029/97JD02012, 1997.

Fischer, H., Birk, M., Blom, C., Carli, B., Carlotti, M., von Clarmann, T., Delbouille, L., Dudhia, A., Ehhalt, D., Endemann, M., Flaud, J. M., Gessner, R., Kleinert, A., Koopman, R., Langen, J., López-Puertas, M., Mosner, P., Nett, H., Oelhaf, H., Perron, G., Remedios, J., Ridolfi, M., Stiller, G., and Zander, R.: MIPAS: an instrument for atmospheric and climate research, Atmospheric Chemistry and Physics, 8, 2151–2188, https://doi.org/10.5194/acp-8-2151-2008, https://www.atmos-chem-phys.net/8/2151/2008/, 2008.

Friedl-Vallon, F., Gulde, T., Hase, F., Kleinert, A., Kulessa, T., Maucher, G., Neubert, T., Olschewski, F., Piesch, C., Preusse, P., Rongen, H., Sartorius, C., Schneider, H., Schönfeld, A., Tan, V., Bayer, N., Blank, J., Dapp, R., Ebersoldt, A., Fischer, H., Graf, F., Guggenmoser, T., Höpfner, M., Kaufmann, M., Kretschmer, E., Latzko, T., Nordmeyer, H., Oelhaf, H., Orphal, J., Riese, M., Schardt, G., Schillings, J., Sha, M. K., Suminska-Ebersoldt, O., and Ungermann, J.: Instrument concept of the imaging Fourier transform spectrometer GLORIA, Atmospheric Measurement Techniques, 7, 3565–3577, https://doi.org/10.5194/amt-7-3565-2014, 2014.

Gelaro, R., McCarty, W., Suárez, M. J., Todling, R., Molod, A., Takacs, L., Randles, C. A., Darmenov, A., Bosilovich, M. G., Reichle, R., Wargan, K., Coy, L., Cullather, R., Draper, C., Akella, S., Buchard, V., Conaty, A., da Silva, A. M., Gu, W., Kim, G.-K., Koster, R., Lucchesi, R., Merkova, D., Nielsen, J. E., Partyka, G., Pawson, S., Putman, W., Rienecker, M., Schubert, S. D., Sienkiewicz, M., and Zhao, B.: The Modern-Era Retrospective Analysis for Research and Applications, Version 2 (MERRA-2), Journal of Climate, 30, 5419–5454, https://doi.org/10.1175/JCLI-D-16-0758.1, https://doi.org/10.1175/JCLI-D-16-0758.1, 2017.

Gettelman, A., Hoor, P., Pan, L. L., Randel, W. J., Hegglin, M. I., and Birner, T.: THE EXTRATROPICAL UPPER TROPOSPHERE AND LOWER STRATOSPHERE, Reviews of Geophysics, 49, https://doi.org/10.1029/2011RG000355, https://agupubs.onlinelibrary.wiley.com/doi/abs/10.1029/2011RG000355, 2011.

Grooß, J.-U., Günther, G., Müller, R., Konopka, P., Bausch, S., Schlager, H., Voigt, C., Volk, C. M., and Toon, G. C.: Simulation of denitrification and ozone loss for the Arctic winter 2002/2003, Atmospheric Chemistry and Physics, 5, 1437–1448, https://doi.org/10.5194/acp-5-1437-2005, 2005.

Grooß, J.-U., Engel, I., Borrmann, S., Frey, W., Günther, G., Hoyle, C. R., Kivi, R., Luo, B. P., Molleker, S., Peter, T., Pitts, M. C., Schlager, H., Stiller, G., Vömel, H., Walker, K. A., and Müller, R.: Nitric acid trihydrate nucleation and denitrification in the Arctic stratosphere, Atmospheric Chemistry and Physics, 14, 1055–1073, https://doi.org/10.5194/acp-14-1055-2014, 2014.

Hübler, G., Fahey, D. W., Kelly, K. K., Montzka, D. D., Carroll, M. A., Tuck, A. F., Heidt, L. E., Pollock, W. H., Gregory, G. L., and Vedder, J. F.: Redistribution of reactive odd nitrogen in the lower Arctic stratosphere, Geophysical Research Letters, 17, 453–456, https://doi.org/10.1029/GL017i004p00453, https://agupubs.onlinelibrary.wiley.com/doi/abs/10.1029/GL017i004p00453, 1990.

Höpfner, M., Larsen, N., Spang, R., Luo, B. P., Ma, J., Svendsen, S. H., Eckermann, S. D., Knudsen, B., Massoli, P., Cairo, F., Stiller, G., v. Clarmann, T., and Fischer, H.: MIPAS detects Antarctic stratospheric belt of NAT PSCs caused by mountain waves, Atmospheric Chemistry and Physics, 6, 1221–1230, https://doi.org/10.5194/acp-6-1221-2006, https://www.atmos-chem-phys.net/6/1221/2006/, 2006.

Hoyle, C. R., Engel, I., Luo, B. P., Pitts, M. C., Poole, L. R., Groo, J.-U., and Peter, T.: Heterogeneous formation of polar stratospheric clouds - Part 1: Nucleation of nitric acid trihydrate (NAT), Atmospheric Chemistry and Physics, 13, 9577–9595, https://doi.org/10.5194/acp-13-9577-2013, 2013.

Höpfner, M., Blom, C. E., Echle, G., Glatthor, N., Hase, F., Stiller, G. P., Karlsruhe, F., and Karlsruhe, U.: G.: Retrieval simulations for MIPAS-STR measurements, in: Hrsg.] IRS 2000: Current Problems in Atmospheric Radiation; Proc.of the Internat. Radiation Symp., St.Petersburg, DEEPAK Publ, 2001.

Jin, J. J., Semeniuk, K., Manney, G. L., Jonsson, A. I., Beagley, S. R., McConnell, J. C., Rinsland, C. P., Boone, C. D., Walker, K. A., and Bernath, P. F.: Denitrification in the Arctic winter 2004/2005: Observations from ACE-FTS, Geophysical Research Letters, 33, L15S01, https://doi.org/10.1029/2006GL027687, 2006.

Johansson, S., Woiwode, W., Höpfner, M., Friedl-Vallon, F., Kleinert, A., Kretschmer, E., Latzko, T., Orphal, J., Preusse, P., Ungermann, J., Santee, M. L., Jurkat-Witschas, T., Marsing, A., Voigt, C., Giez, A., Krämer, M., Rolf, C., Zahn, A., Engel, A., Sinnhuber, B.-M., and Oelhaf, H.: Airborne limb-imaging measurements of temperature, HNO_3, O_3, $ClONO_2$, H_2O and CFC-12 during the Arctic winter 2015/2016: characterization, in situ validation and comparison to Aura/MLS, Atmospheric Measurement Techniques, 11, 4737–4756, https://doi.org/10.5194/amt-11-4737-2018, https://www.atmos-meas-tech.net/11/4737/2018/, 2018.

Johansson, S.~~e. a.~~, Santee, M. L., Grooß, J.-U., Höpfner, M., Braun, M., Friedl-Vallon, F., Khosrawi, F., Kirner, O., Kretschmer, E., Oelhaf, H., Orphal, J., Sinnhuber, B.-M., Tritscher, I., Ungermann, J., Walker, K. A., and Woiwode, W.: Unusual chlorine partitioning in the 2015/16 Arctic winter lowermost stratosphere: Observations and simulations, Atmospheric Chemistry and Physics Discussions, ~~2018, 2018b.~~ 2019, 1–38, https://doi.org/10.5194/acp-2018-1227, https://www.atmos-chem-phys-discuss.net/acp-2018-1227/, 2019.

Khosrawi, F., Urban, J., Pitts, M. C., Voelger, P., Achtert, P., Kaphlanov, M., Santee, M. L., Manney, G. L., Murtagh, D., and Fricke, K.-H.: Denitrification and polar stratospheric cloud formation during the Arctic winter 2009/2010, Atmospheric Chemistry and Physics, 11, 8471–8487, https://doi.org/10.5194/acp-11-8471-2011, 2011.

Khosrawi, F., Kirner, O., Sinnhuber, B.-M., Johansson, S., ~~Höpfner~~Höpfner, M., Santee, M. L., Froidevaux, L., Ungermann, J., Ruhnke, R., Woiwode, W., Oelhaf, H., and Braesicke, P.: Denitrification, dehydration and ozone loss during the ~~Arctic winter~~ 2015/2016 ~~,~~ Arctic

winter, Atmospheric Chemistry and PhysicsDiscussions, pp. 1–33, , , 17, 12 893–12 910, https://doi.org/10.5194/acp-17-12893-2017, https://www.atmos-chem-phys.net/17/12893/2017/, 2017.

Kim, Y., Choi, W., Lee, K., Park, J. H., Massie, S. T., Sasano, Y., Nakajima, H., and Yokota, T.: Polar stratospheric clouds observed by the ILAS-II in the Antarctic region: Dual compositions and variation of compositions during June to August of 2003, Journal of Geophysical Research: Atmospheres, 111, https://doi.org/10.1029/2005JD006445, https://agupubs.onlinelibrary.wiley.com/doi/abs/10.1029/2005JD006445, 2006.

Kleinert, A., Friedl-Vallon, F., Guggenmoser, T., Höpfner, M., Neubert, T., Ribalda, R., Sha, M. K., Ungermann, J., Blank, J., Ebersoldt, A., Kretschmer, E., Latzko, T., Oelhaf, H., Olschewski, F., and Preusse, P.: Level 0 to 1 processing of the imaging Fourier transform spectrometer GLORIA: generation of radiometrically and spectrally calibrated spectra, Atmospheric Measurement Techniques, 7, 4167–4184, https://doi.org/10.5194/amt-7-4167-2014, https://www.atmos-meas-tech.net/7/4167/2014/, 2014.

Krause, J., Hoor, P., Engel, A., Plöger, F., Grooß, J.-U., Bönisch, H., Keber, T., Sinnhuber, B.-M., Woiwode, W., and Oelhaf, H.: Mixing and ageing in the polar lower stratosphere in winter 2015–2016, Atmospheric Chemistry and Physics, 18, 6057–6073, https://doi.org/10.5194/acp-18-6057-2018, https://www.atmos-chem-phys.net/18/6057/2018/, 2018.

Manney, G. L. and Lawrence, Z. D.: The major stratospheric final warming in 2016: Dispersal of vortex air and termination of Arctic chemical ozone loss, Atmospheric Chemistry and Physics, 16, 15 371–15 396, https://doi.org/10.5194/acp-16-15371-2016, 2016.

Manney, G. L., Zurek, R. W., O'Neill, A., and Swinbank, R.: On the Motion of Air through the Stratospheric Polar Vortex, Journal of the Atmospheric Sciences, 51, 2973–2994, https://doi.org/10.1175/1520-0469(1994)051<2973:OTMOAT>2.0.CO;2, 1994.

Matthias, V., Dörnbrack, A., and Stober, G.: The extraordinarily strong and cold polar vortex in the early northern winter 2015/2016, Geophysical Research Letters, 43, 12,287–12,294, https://doi.org/10.1002/2016GL071676, 2016.

McKenna, D. S.: A new Chemical Lagrangian Model of the Stratosphere (CLaMS) 1. Formulation of advection and mixing, Journal of Geophysical Research, 107, 1435, https://doi.org/10.1029/2000JD000114, 2002a.

McKenna, D. S.: A new Chemical Lagrangian Model of the Stratosphere (CLaMS) 2. Formulation of chemistry scheme and initialization, Journal of Geophysical Research, 107, https://doi.org/10.1029/2000JD000113, 2002b.

Molleker, S., Borrmann, S., Schlager, H., Luo, B., Frey, W., Klingebiel, M., Weigel, R., Ebert, M., Mitev, V., Matthey, R., Woiwode, W., Oelhaf, H., Dörnbrack, A., Stratmann, G., Grooß, J.-U., Günther, G., Vogel, B., Müller, R., Krämer, M., Meyer, J., and Cairo, F.: Microphysical properties of synoptic-scale polar stratospheric clouds: In situ measurements of unexpectedly large HNO₃-containing particles in the Arctic vortex, Atmospheric Chemistry and Physics, 14, 10 785–10 801, https://doi.org/10.5194/acp-14-10785-2014, 2014.

Nash, E. R., Newman, P. A., Rosenfield, J. E., and Schoeberl, M. R.: An objective determination of the polar vortex using Ertel's potential vorticity, Journal of Geophysical Research: Atmospheres, 101, 9471–9478, https://doi.org/10.1029/96JD00066, 1996.

Northway, M. J., Gao, R. S., Popp, P. J., Holecek, J. C., Fahey, D. W., Carslaw, K. S., Tolbert, M. A., Lait, L. R., Dhaniyala, S., Flagan, R. C., Wennberg, P. O., Mahoney, M. J., Herman, R. L., Toon, G. C., and Bui, T. P.: An analysis of large HNO_3-containing particles sampled in the Arctic stratosphere during the winter of 1999/2000, Journal of Geophysical Research: Atmospheres, 107, SOL 41–1–SOL 41–22, https://doi.org/10.1029/2001JD001079, https://agupubs.onlinelibrary.wiley.com/doi/abs/10.1029/2001JD001079, 2002.

Pitts, M. C., Poole, L. R., and Gonzalez, R.: Polar stratospheric cloud climatology based on CALIPSO spaceborne lidar measurements from 2006 to 2017, Atmospheric Chemistry and Physics, 18, 10 881–10 913, https://doi.org/10.5194/acp-18-10881-2018, https://www.atmos-chem-phys.net/18/10881/2018/, 2018.

Popp, P. J., Northway, M. J., Holecek, J. C., Gao, R. S., Fahey, D. W., Elkins, J. W., Hurst, D. F., Romashkin, P. A., Toon, G. C., Sen, B., Schauffler, S. M., Salawitch, R. J., Webster, C. R., Herman, R. L., Jost, H., Bui, T. P., Newman, P. A., and Lait, L. R.: Severe and extensive denitrification in the 1999-2000 Arctic winter stratosphere, Geophysical Research Letters, 28, 2875–2878, https://doi.org/10.1029/2001GL013132, 2001.

Rex, M., Salawitch, R. J., Deckelmann, H., von der Gathen, P., Harris, N. R. P., Chipperfield, M. P., Naujokat, B., Reimer, E., Allaart, M., Andersen, S. B., Bevilacqua, R., Braathen, G. O., Claude, H., Davies, J., de Backer, H., Dier, H., Dorokhov, V., Fast, H., Gerding, M., Godin-Beekmann, S., Hoppel, K., Johnson, B., Kyrö, E., Litynska, Z., Moore, D., Nakane, H., Parrondo, M. C., Risley, A. D., Skrivankova, P., Stübi, R., Viatte, P., Yushkov, V., and Zerefos, C.: Arctic winter 2005: Implications for stratospheric ozone loss and climate change, Geophysical Research Letters, 33, 221, https://doi.org/10.1029/2006GL026731, 2006.

Riese, M., Ploeger, F., Rap, A., Vogel, B., Konopka, P., Dameris, M., and Forster, P.: Impact of uncertainties in atmospheric mixing on simulated UTLS composition and related radiative effects, Journal of Geophysical Research: Atmospheres, 117, n/a–n/a, https://doi.org/10.1029/2012JD017751, 2012.

Riese, M., Oelhaf, H., Preusse, P., Blank, J., Ern, M., Friedl-Vallon, F., Fischer, H., Guggenmoser, T., Höpfner, M., Hoor, P., Kaufmann, M., Orphal, J., Plöger, F., Spang, R., Suminska-Ebersoldt, O., Ungermann, J., Vogel, B., and Woiwode, W.: Gimballed Limb Observer for Radiance Imaging of the Atmosphere (GLORIA) scientific objectives, Atmospheric Measurement Techniques, 7, 1915–1928, https://doi.org/10.5194/amt-7-1915-2014, 2014.

Santee, M. L., Manney, G. L., Froidevaux, L., Read, W. G., and Waters, J. W.: Six years of UARS Microwave Limb Sounder HNO3 observations: Seasonal, interhemispheric, and interannual variations in the lower stratosphere, Journal of Geophysical Research: Atmospheres, 104, 8225–8246, https://doi.org/10.1029/1998JD100089, https://agupubs.onlinelibrary.wiley.com/doi/abs/10.1029/1998JD100089, 1999.

Sinnhuber, B.-M., Stiller, G., Ruhnke, R., von Clarmann, T., Kellmann, S., and Aschmann, J.: Arctic winter 2010/2011 at the brink of an ozone hole, Geophysical Research Letters, 38, https://doi.org/10.1029/2011GL049784, 2011.

Stiller, G. P., von Clarmann, T., Funke, B., Glatthor, N., Hase, F., Höpfner, M., and Linden, A.: Sensitivity of trace gas abundances retrievals from infrared limb emission spectra to simplifying approximations in radiative transfer modelling, Journal of Quantitative Spectroscopy and Radiative Transfer, 72, 249 – 280, https://doi.org/https://doi.org/10.1016/S0022-4073(01)00123-6, http://www.sciencedirect.com/science/article/pii/S0022407301001236, 2002.

Stratmann, G., Ziereis, H., Stock, P., Brenninkmeijer, C., Zahn, A., Rauthe-Schöch, A., Velthoven, P., Schlager, H., and Volz-Thomas, A.: NO and NOy in the upper troposphere: Nine years of CARIBIC measurements onboard a passenger aircraft, Atmospheric Environment, 133, 93 – 111, https://doi.org/https://doi.org/10.1016/j.atmosenv.2016.02.035, http://www.sciencedirect.com/science/article/pii/S1352231016301480, 2016.

Tabazadeh, A. and Toon, O. B.: The presence of metastable HNO_3/H_2O solid phases in the stratosphere inferred from ER 2 data, Journal of Geophysical Research: Atmospheres, 101, 9071–9078, https://doi.org/10.1029/96JD00062, 1996.

Tritscher, I., Grooß, J.-U., Spang, R., Pitts, M. C., Poole, L. R., Müller, R., and Riese, M.: Lagrangian simulation of ice particles and resulting dehydration in the polar winter stratosphere, Atmospheric Chemistry and Physics~~Discussions, 2018, 1–32,~~, 19, 543–563, https://doi.org/10.5194/acp-19-543-2019, ~~, 2018.~~ https://www.atmos-chem-phys.net/19/543/2019/, 2019.

Tuck, A. F., Baumgardner, D., Chan, K. R., Dye, J. E., Elkins, J. W., Hovde, S. J., Kelly, K. K., Loewenstein, M., Margitan, J. J., May, R. D., Podolske, J. R., Proffitt, M. H., Rosenlof, K. H., Smith, W. L., Webster, C. R., and Wilson, J. C.: The Brewer-Dobson

Circulation In the Light of High Altitude In Situ Aircraft Observations, Quarterly Journal of the Royal Meteorological Society, 123, 1–69, https://doi.org/10.1002/qj.49712353702, https://doi.org/10.1002/qj.49712353702, 1997.

Voigt, C., Dörnbrack, A., Wirth, M., Groß, S. M., Pitts, M. C., Poole, L. R., Baumann, R., Ehard, B., Sinnhuber, B.-M., Woiwode, W., and Oelhaf, H.: Widespread polar stratospheric ice clouds in the 2015–2016 Arctic winter – implications for ice nucleation, Atmospheric Chemistry and Physics, 18, 15 623–15 641, https://doi.org/10.5194/acp-18-15623-2018, https://www.atmos-chem-phys.net/18/15623/2018/, 2018.

Waibel, A. E.: Arctic Ozone Loss Due to Denitrification, Science (New York, N.Y.), 283, 2064–2069, https://doi.org/10.1126/science.283.5410.2064, 1999.

Waters, J. W., Froidevaux, L., Harwood, R. S., Jarnot, R. F., Pickett, H. M., Read, W. G., Siegel, P. H., Cofield, R. E., Filipiak, M. J., Flower, D. A., Holden, J. R., Lau, G. K., Livesey, N. J., Manney, G. L., Pumphrey, H. C., Santee, M. L., Wu, D. L., Cuddy, D. T., Lay, R. R., Loo, M. S., Perun, V. S., Schwartz, M. J., Stek, P. C., Thurstans, R. P., Boyles, M. A., Chandra, K. M., Chavez, M. C., Chen, G.-S., Chudasama, B. V., Dodge, R., Fuller, R. A., Girard, M. A., Jiang, J. H., Jiang, Y., Knosp, B. W., LaBelle, R. C., Lam, J. C., Lee, K. A., Miller, D., Oswald, J. E., Patel, N. C., Pukala, D. M., Quintero, O., Scaff, D. M., van Snyder, W., Tope, M. C., Wagner, P. A., and Walch, M. J.: The Earth observing system microwave limb sounder (EOS MLS) on the aura Satellite, IEEE Transactions on Geoscience and Remote Sensing, 44, 1075–1092, https://doi.org/10.1109/TGRS.2006.873771, 2006.

Werner, A., Volk, C. M., Ivanova, E. V., Wetter, T., Schiller, C., Schlager, H., and Konopka, P.: Quantifying transport into the Arctic lowermost stratosphere, Atmospheric Chemistry and Physics, 10, 11 623–11 639, https://doi.org/10.5194/acp-10-11623-2010, https://www.atmos-chem-phys.net/10/11623/2010/, 2010.

Woiwode, W., Grooß, J.-U., Oelhaf, H., Molleker, S., Borrmann, S., Ebersoldt, A., Frey, W., Gulde, T., Khaykin, S., Maucher, G., Piesch, C., and Orphal, J.: Denitrification by large NAT particles: The impact of reduced settling velocities and hints on particle characteristics, Atmospheric Chemistry and Physics, 14, 11 525–11 544, https://doi.org/10.5194/acp-14-11525-2014, 2014.

Woiwode, W., Höpfner, M., Bi, L., Pitts, M. C., Poole, L. R., Oelhaf, H., Molleker, S., Borrmann, S., Klingebiel, M., Belyaev, G., Ebersoldt, A., Griessbach, S., Grooß, J.-U., Gulde, T., Krämer, M., Maucher, G., Piesch, C., Rolf, C., Sartorius, C., Spang, R., and Orphal, J.: Spectroscopic evidence of large aspherical β-NAT particles involved in denitrification in the December 2011 Arctic stratosphere, Atmospheric Chemistry and Physics, 16, 9505–9532, https://doi.org/10.5194/acp-16-9505-2016, 2016.

Zhu, Y., Toon, O. B., Pitts, M. C., Lambert, A., Bardeen, C., and Kinnison, D. E.: Comparing simulated PSC optical properties with CALIPSO observations during the 2010 Antarctic winter, Journal of Geophysical Research: Atmospheres, 122, 1175–1202, https://doi.org/10.1002/2016JD025191, https://agupubs.onlinelibrary.wiley.com/doi/abs/10.1002/2016JD025191, 2017.

Ziereis, H., Minikin, A., Schlager, H., Gayet, J. F., Auriol, F., Stock, P., Baehr, J., Petzold, A., Schumann, U., Weinheimer, A., Ridley, B., and Ström, J.: Uptake of reactive nitrogen on cirrus cloud particles during INCA, Geophysical Research Letters, 31, https://doi.org/10.1029/2003GL018794, https://agupubs.onlinelibrary.wiley.com/doi/abs/10.1029/2003GL018794, 2004.